Physical and Chemical Properties of Atmospheric Pollution in Megacities

Maria de Fátima Andrade
Departamento de Ciências Atmosféricas
Instituto de Astronomia, Geofísica e Ciências Atmosféricas
Universidade de Sao Paulo

Chemical Composition of Atmosphere

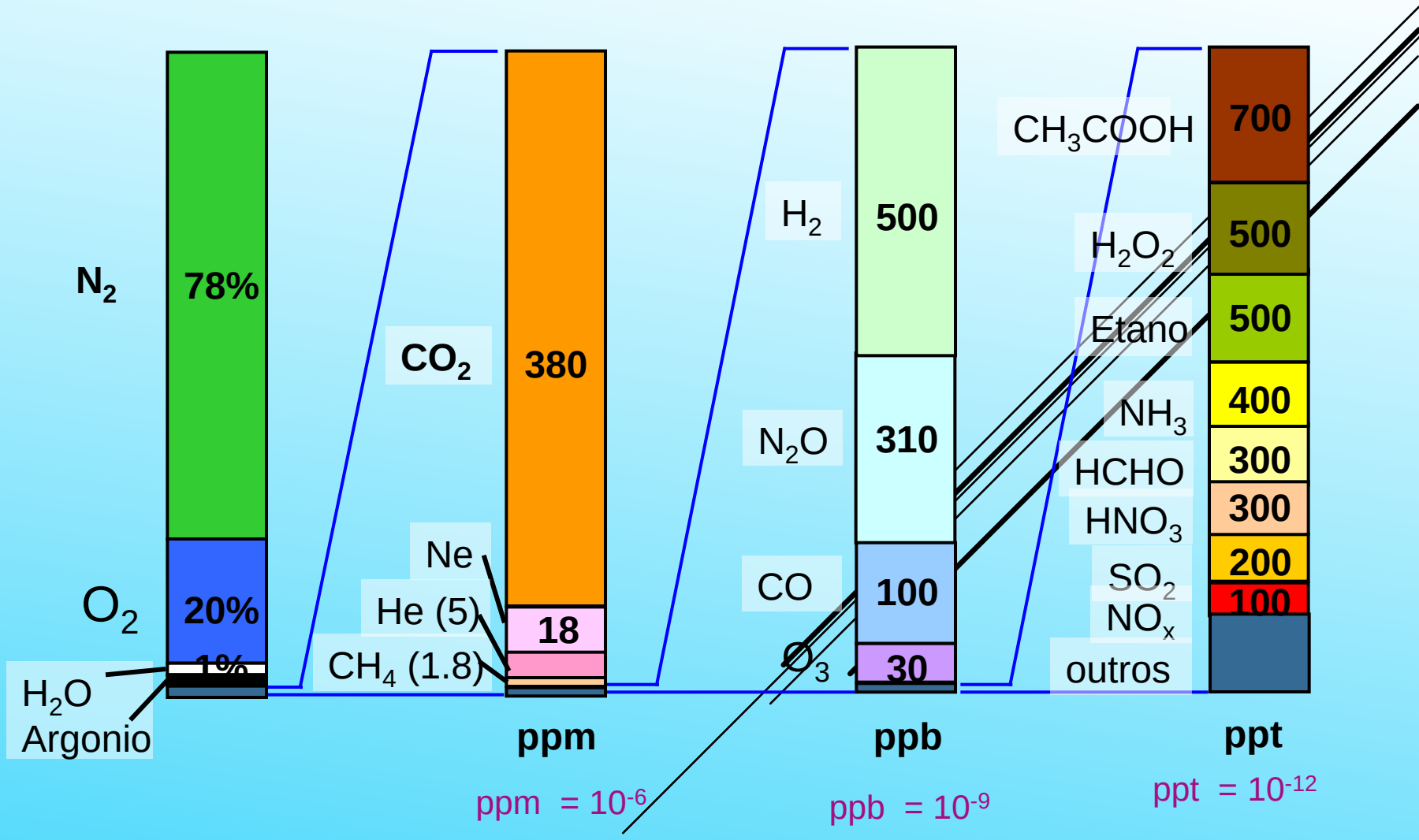

Regulated pollutants: O3, NO2, SO2, MP

Radiative Forcing – IPCC, AR5

GHG

SLCP

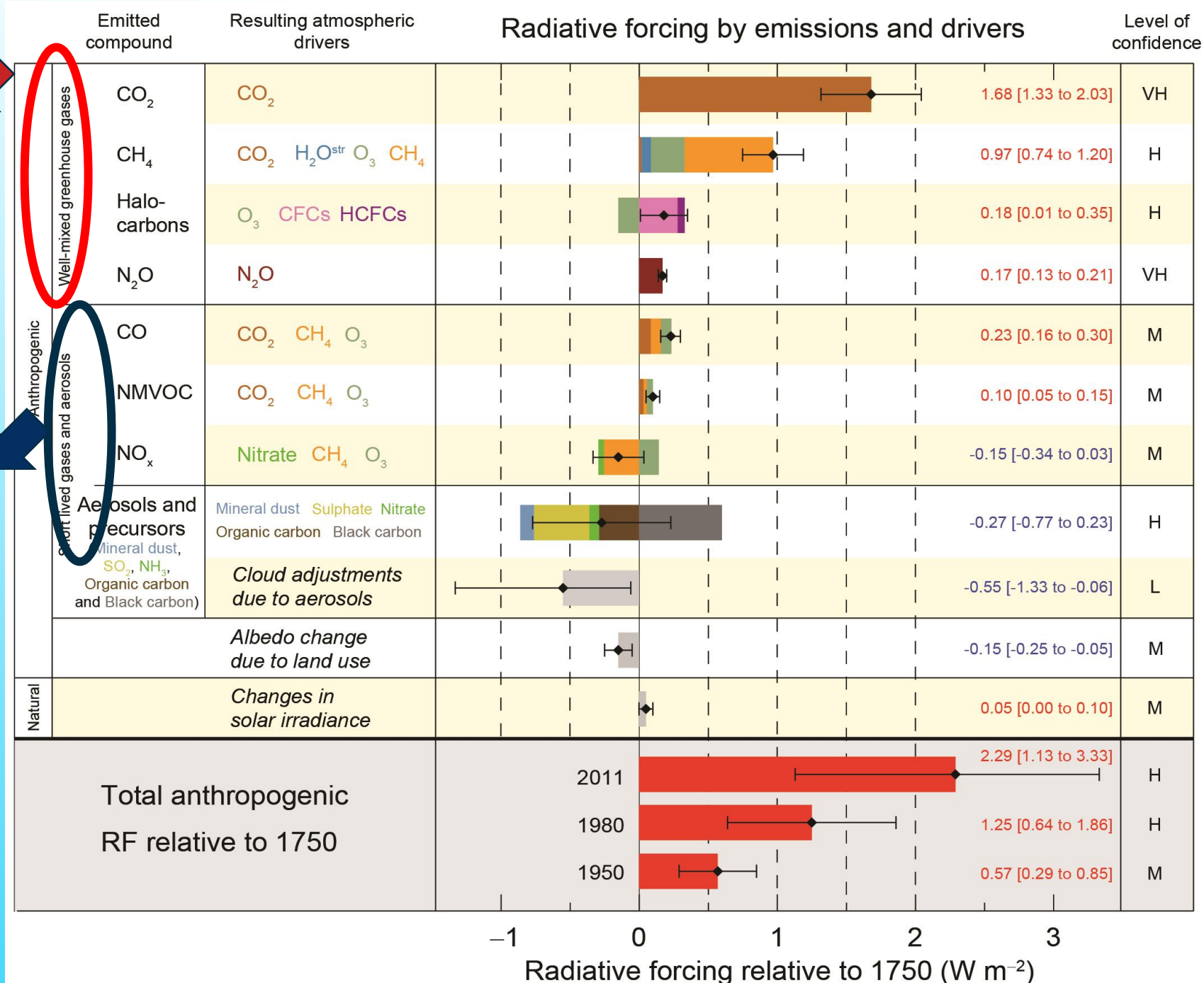

MAIN AIR POLLUTION PROBLEMS

- $PM_{2.5}$
  - Secondary organic formation
  - Secondary inorganic formation

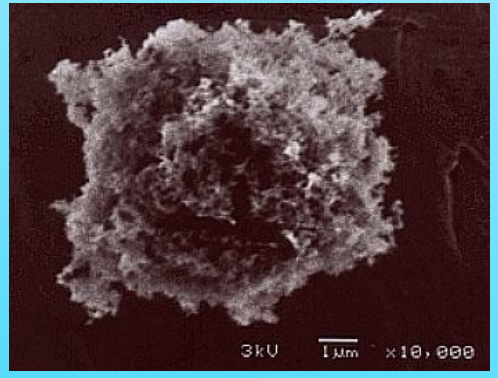

- OZONE
  - Contribution of ethanol fuel
  - Contribution of gasohol
  - Evaporative emissions

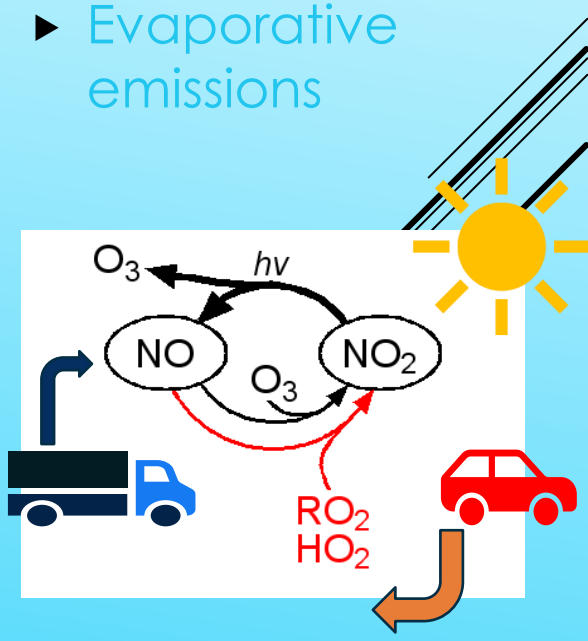

AIR POLLUTION REDUCTIONS

People in The Americas are breathing cleaner air than 5 years ago

60%

About 60% of urban residents in low- and middle-income countries in the Region of the Americas are breathing cleaner air than they did 5 years ago, about the same progress seen in high-income countries in the Region of the Americas.

BREATHELIFE
Clean air. Healthy future.

World Health Organization

CLIMATE & CLEAN AIR COALITION
TO REDUCE SHORT-LIVED CLIMATE POLLUTANTS

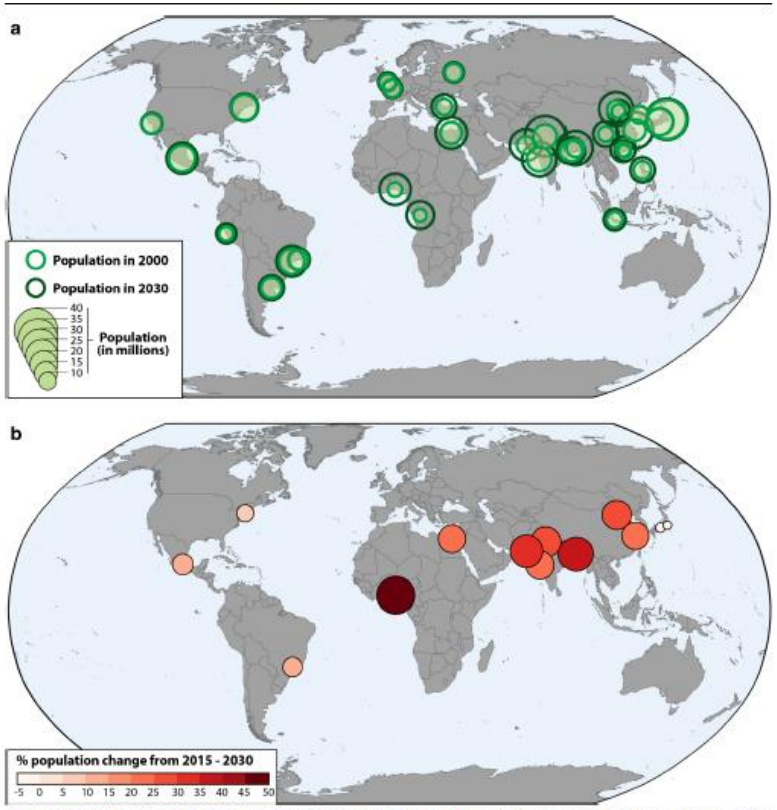

Fig. 1 a Population in the 30 most populous megacities for 2000–2030, with projected 2030 population indicated by *darker colors* and b % population change from 2015 to 2030 for the 10 most populous cities in both years (given overlap, this amounts to 13 cities total) [2]

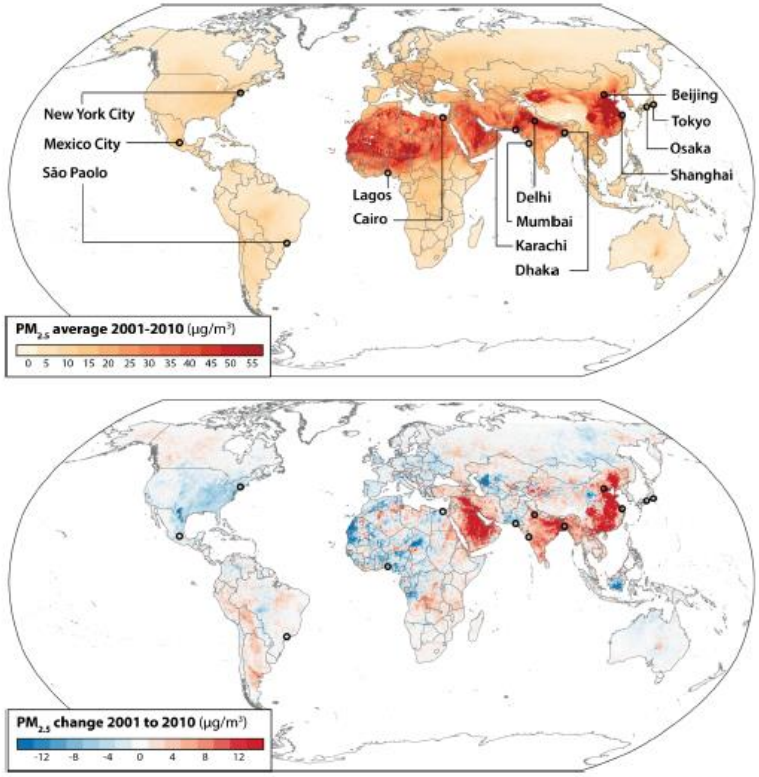

Fig. 2 Global average satellite-derived $PM_{2.5}$ from 2001 to 2010 (µg/m^3), including dust (*top panel*) and the change from 2001 to 2010 (*bottom panel*). 2001 and 2010 estimates were selected from datasets as the center of a 3-year average (2000–2002 for 2001) [6, 7••]. Most populous megacities (defined for 2015 and 2030 projections) are indicated on the map

Curr Clim Change Rep (2016) 2:15–27

Annual average $PM_{2.5}$ concentration in cities estimated from surface monitoring and GBD2010 model

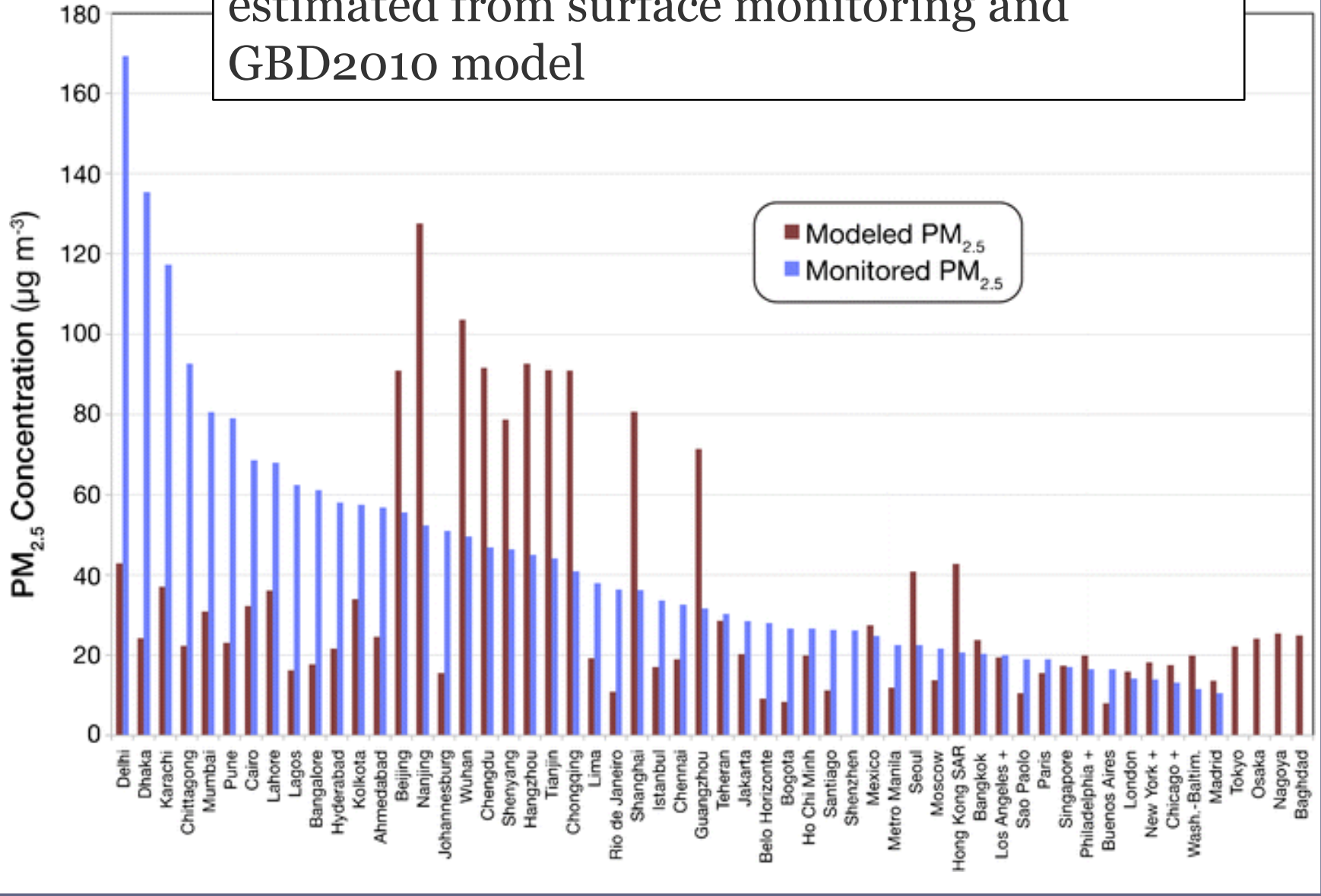

•Krzyzanowski, 2014

$PM_{2.5}$ exposure estimates used in GBD2010 analysis were based on a combination of estimates provided by global chemical transport model TM5, and estimates from remote sensing and calibrated to available surface measurements.

Year 2005 emissions from the GAINS emissions data base.

Satellite-derived $PM_{2.5}$ estimates were based on the observations of the Aerosol Optical Depth (AOD) provided by the National Aeronautics and Space Administration (NASA) from two instruments (MODIS and MISR).

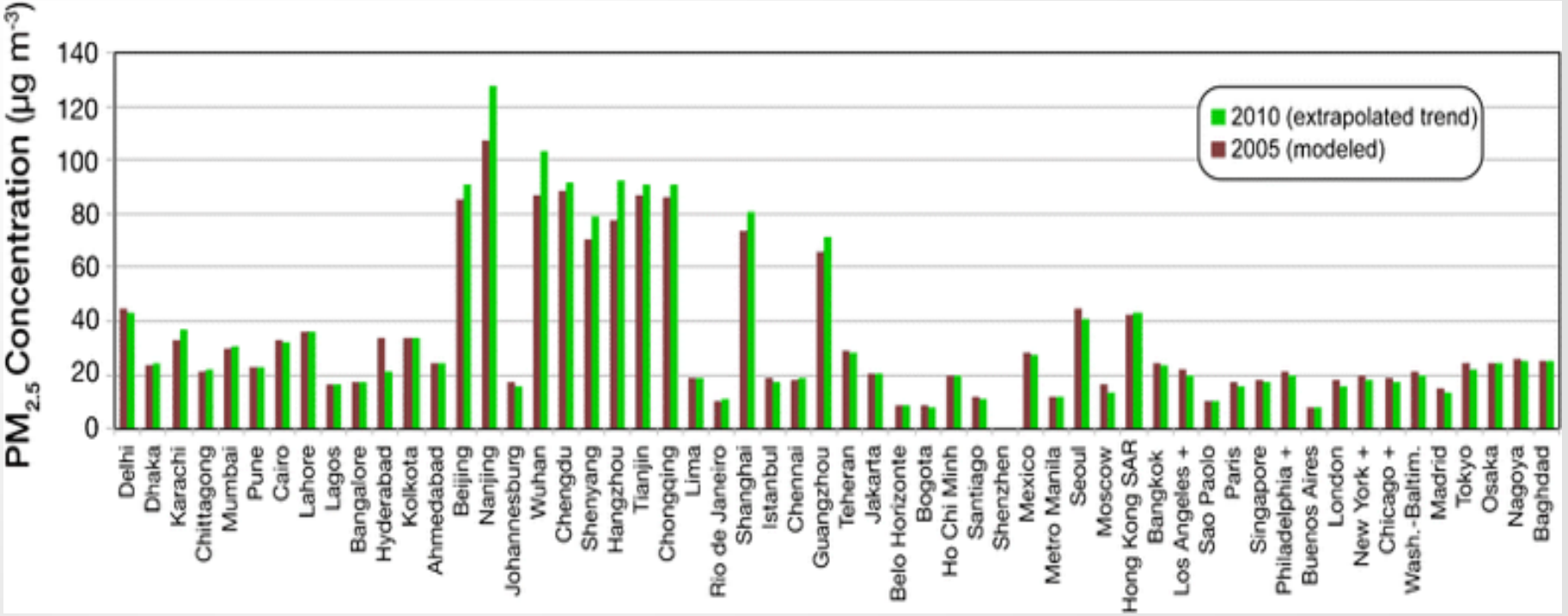

Annual average $PM_{2.5}$ concentration in cities estimated with GBD2010 model for 2005 and extrapolated to 2010

- Krzyzanowski, 2014

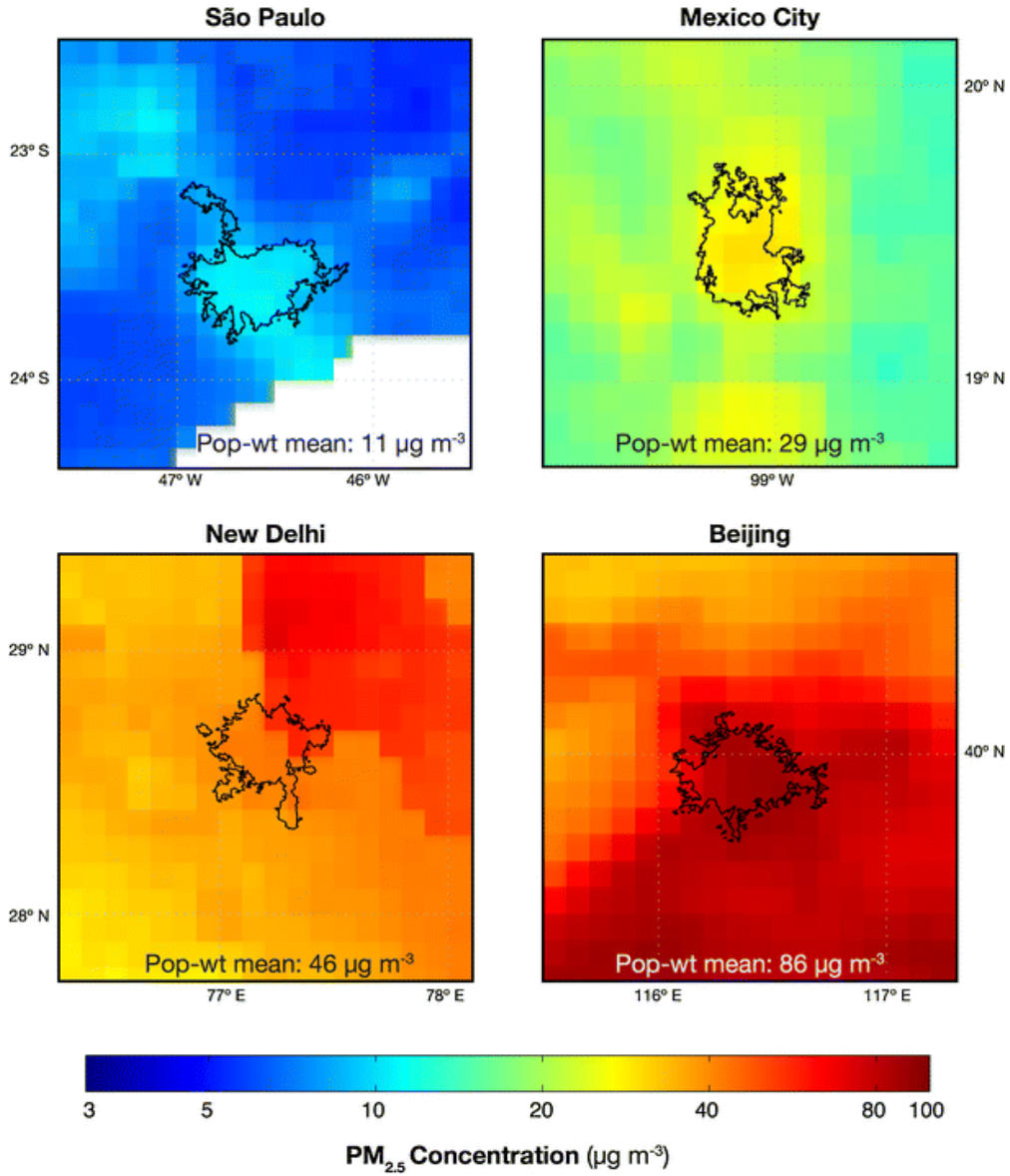

Year 2005 $PM_{2.5}$ surfaces at 0.1° grid resolution for the surrounding environs of four mega-cities (São Paulo, Mexico City, New Delhi and Beijing) derived from a combination of satellite remote sensing, chemical transport modelling, and ground-based observations

The population-weighted mean of the $PM_{2.5}$ surface within the urbanized land area is displayed for each city

Bluer Skies in Beijing

Pollution levels in China's capital fell as the government clamped down on coal burning

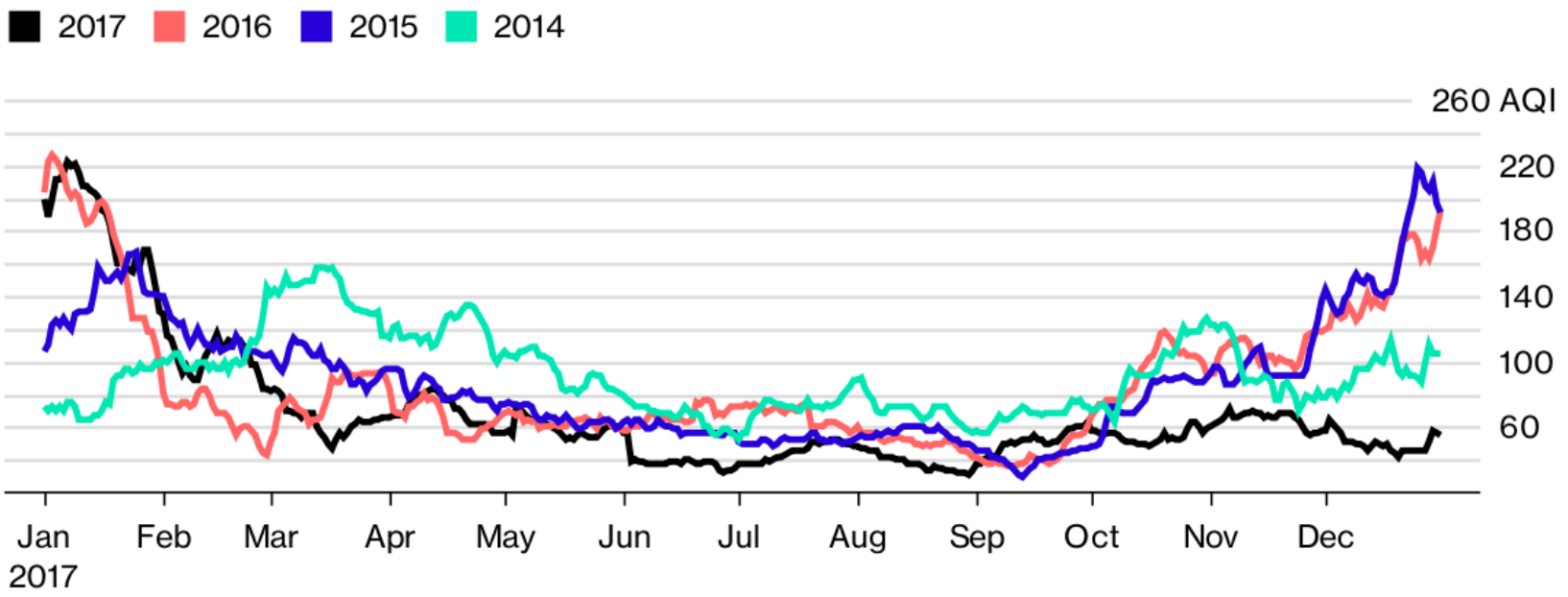

Note: Chart illustrates 30-day moving average of air pollution levels
Source: China Air Quality Index

Bloomberg

Ground-level Ozone Is a Growing Problem in China

Average concentrations of air pollutants in China as percentages higher or lower than national standards

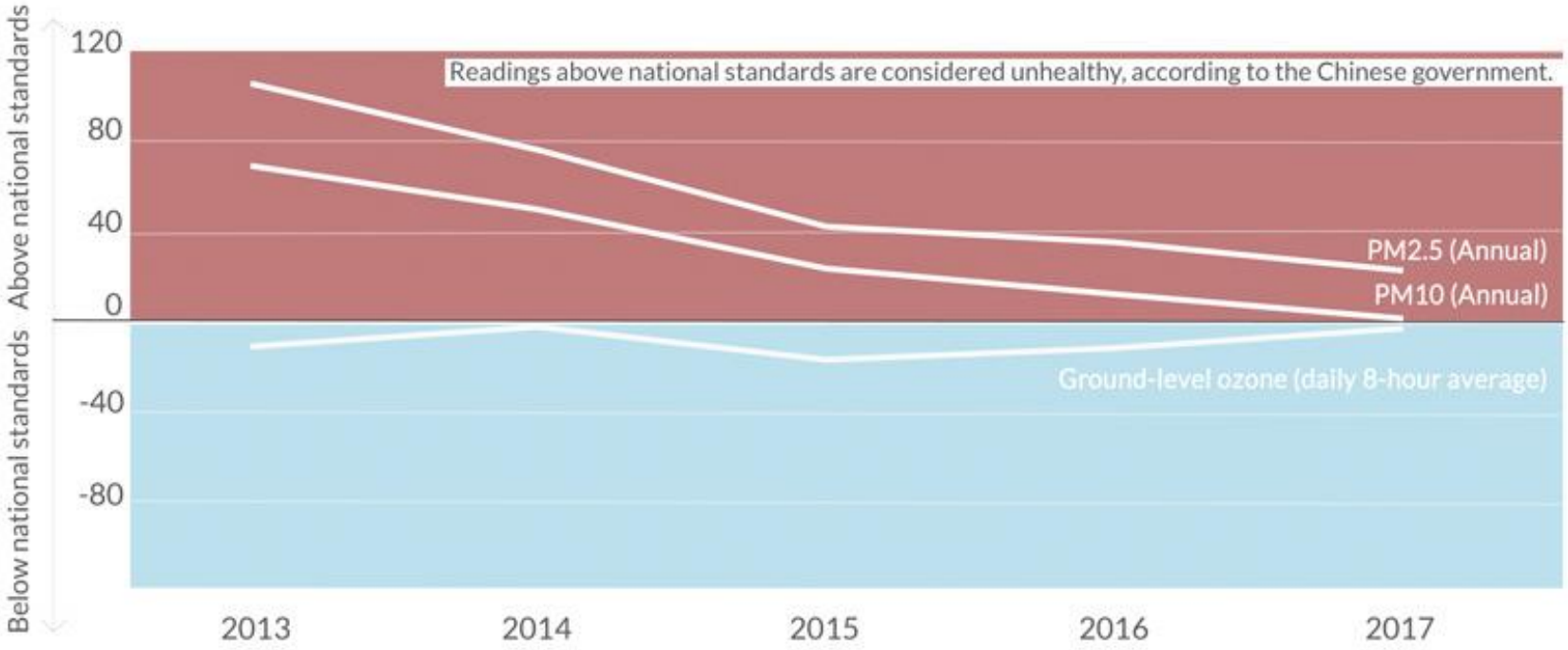

Note Chinese air-quality standards permit higher levels of pollution than WHO standards.

Source: Ministry of Ecology and Environment's 2013-2017 ecological reports.

SIXTH TONE

Li Mengqi

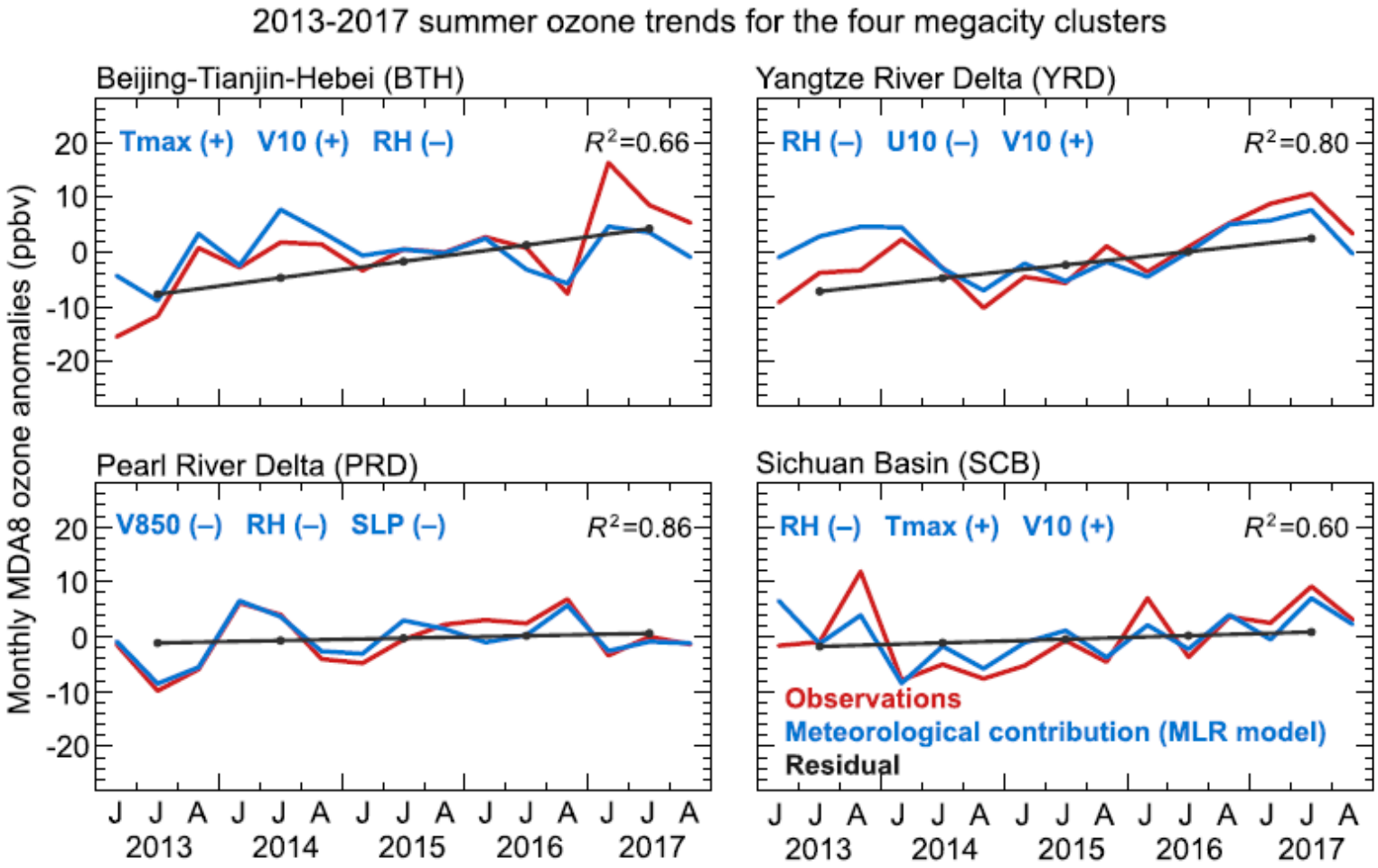

Fig. 2. Time series of monthly mean MDA8 ozone anomalies in summer (JJA) 2013–2017 for the four megacity clusters of Fig. 1: BTH, YRD. PRD, SCB. MDA8 ozone values for individual 0.5° × 0.625° grid cells are averaged over each cluster and month, and anomalies are computed relative to the 2013–2017 means for that month of the year. In each panel, observations (red line) are compared with results from an MLR model driven by meteorological variability (blue line). The linear trend of the 3-mo average residuals for each year is shown in black. The MLR model uses the top three meteorological predictors (Table 1) for each 0.5° × 0.625° grid cell in the cluster, and the results are then averaged for each cluster. The dominant variables in each cluster are indicated in legend with the sign of their correlation to MDA8 ozone. The coefficients of determination (R^2) for the MLR model are shown in the right corner of each plot for the detrended time series (removing the residual linear trend).

PHOTOCHEMISTRY

P. S. Monks et al.: Tropospheric ozone and its precursors

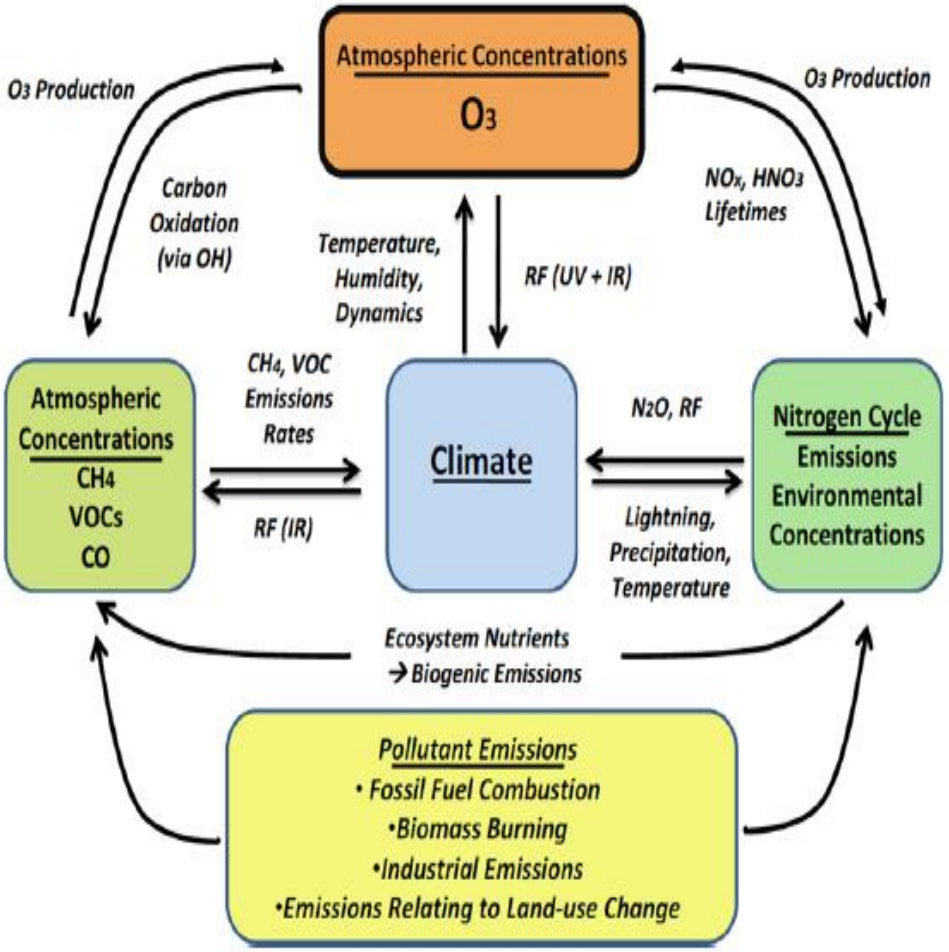

Figure 1. Schematic representation of the interactions of ozone in the Earth system (EPA, 2009).

Atmos. Chem. Phys., 15, 8889–8973, 2015

Table 3.1. Global present-day budget of tropospheric ozone

	Best estimate, Tg O_3 a^{-1}
Sources	
Tropospheric chemical production	4500
Transport from stratosphere	500
Sinks	
Tropospheric chemical loss	4000
Deposition	1000

Estimates based on Wu et al. (2007)

- Ozone Precursors: nitrogen oxides (NOx), carbon monoxide (CO), methane (CH_4), and nonmethane hydrocarbons (NMHC)

- Importance of hydroxyl (OH) and peroxy radicals (HO_2 or RO_2)

PHOTOCHEMISTRY

Atmospheric Chemistry - Tropospheric ozone

$$NO_2 (h\upsilon, \lambda<400\ nm) \rightarrow NO + O$$

$$O + O_2 + M \rightarrow O_3$$

$$ROO^{\bullet} + NO \rightarrow RO^{\bullet} + NO_2$$

$$NO + O_3 \rightarrow NO_2 + O_2$$

Role of VOC on ozone formation

$$COV + OH \xrightarrow{[O_2]} RO_2 + H_2O \cdots\cdots\cdots\cdots\cdots\cdots\cdots\cdots R1$$

$$CO + OH \xrightarrow{[O_2]} HO_2 + CO_2 \cdots\cdots\cdots\cdots\cdots\cdots\cdots\cdots R2$$

$$RO_2 + NO \xrightarrow{[O_2]} COV_{\text{sec}\,undário} + HO_2 + NO_2 \cdots\cdots\cdots\cdots R3$$

$$HO_2 + NO \rightarrow OH + NO_2 \cdots\cdots\cdots\cdots\cdots\cdots\cdots\cdots R4$$

$$NO_2 + h\upsilon \rightarrow NO + O \cdots\cdots\cdots\cdots\cdots\cdots\cdots\cdots R5$$

$$O + O_2 + M \rightarrow O_3 + M \cdots\cdots\cdots\cdots\cdots\cdots\cdots\cdots R6$$

RO_2 represents any organic molecula

At night or close to strong sources of NO

$$NO + O_3 \rightarrow NO_2 + O_2 \cdots\cdots\cdots\cdots\cdots\cdots\cdots\cdots R7$$

RATIO VOC/NOX AND OZONE FORMATION

$NO_2 + h\nu \rightarrow NO + O$

$O + O_2 + M \rightarrow O_3 + M$

$O_3 + NO \rightarrow NO_2 + O_2$

- If no nitrogen oxides are available, the reaction cycle cannot take place.
- If too much nitrogen oxides are available the excess of nitrogen oxide NO reacts not only with the peroxy-radicals but removes the ozone again.
- If no sunlight is available NO cannot be recycled again and the formation of peroxy-radicals is not sufficient.

$O_3 + h\nu \rightarrow O(1D) + O_2$

$O(1D) + H_2O \rightarrow$ **2OH. (the radical hidroxila is the key to understand the tropospheric chemistry)**

$RH + OH. \rightarrow R. + H_2O$

$R. + O_2 \rightarrow RO_2.$

$RO_2.+ NO \rightarrow NO_2 + RO.$

$OH. + NO_2 + M \rightarrow HNO_3 + M$

More VOC

NOx-limitante

More NOx

COV-limitante

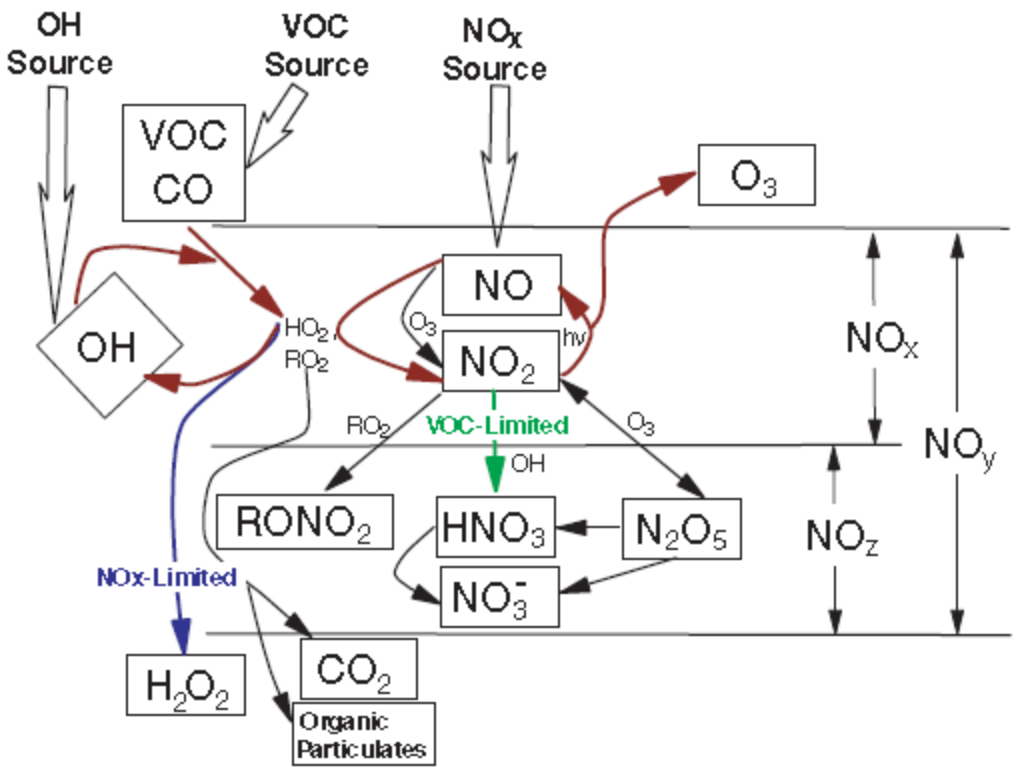

Figure 3.9 Schematic of the photochemical pathways leading to the production of O_3 (red lines) and the termination steps that dominate under NO_x-limited (blue line) and VOC-limited (green line) regimes.

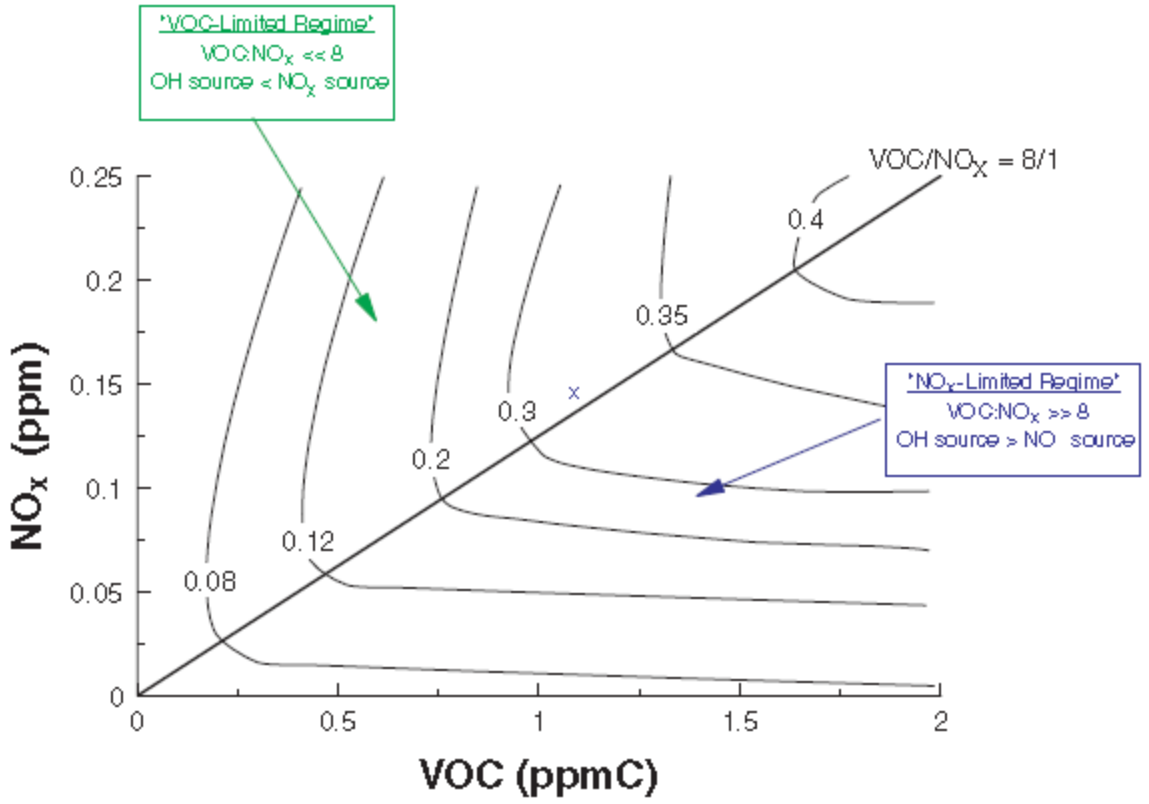

Figure 3.10 Isopleths of 1-hour maximum O_3 concentrations (in ppm) calculated as a function of initial VOC and NO_x concentrations and the regions of the diagram that are characterized by VOC- or NO_x-limitation.

Industrial Area

Urbanl Area

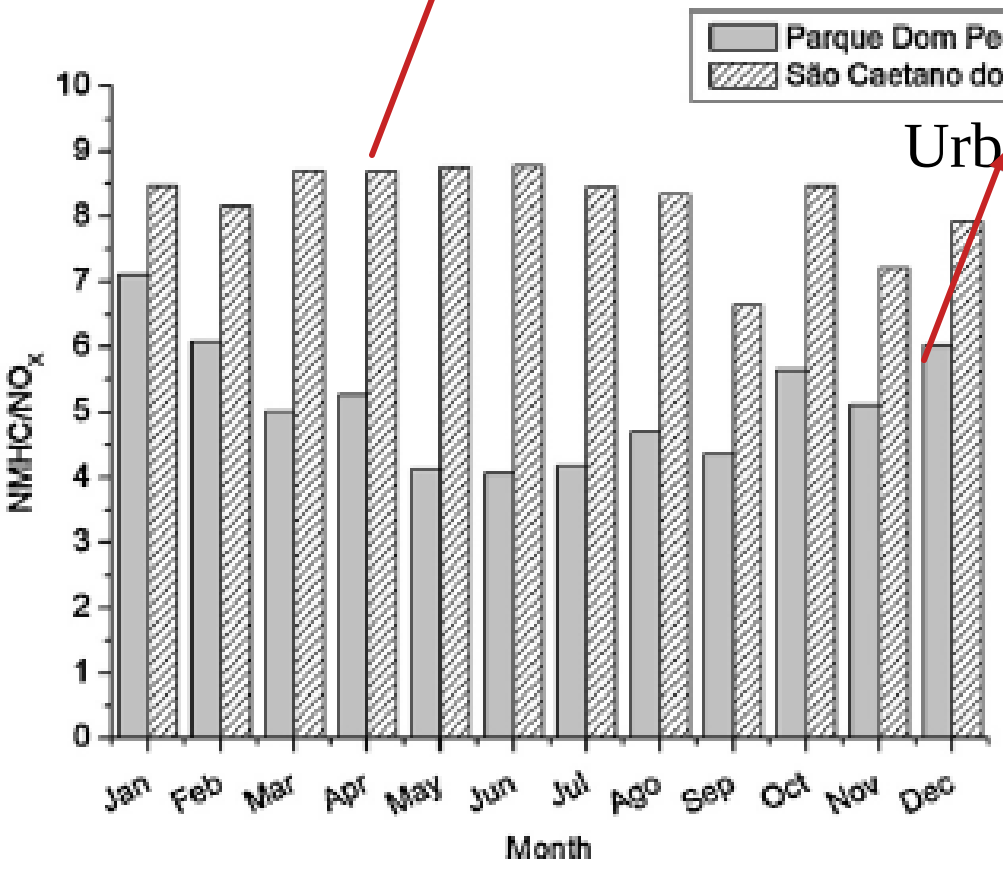

Fig. 8 – Monthly mean (1996–2005) of NMHC/NO_x ratio registered at Parque Dom Pedro II and São Caetano do Sul sites.

Razão NMHC/Nox
7:00-9:00 horas

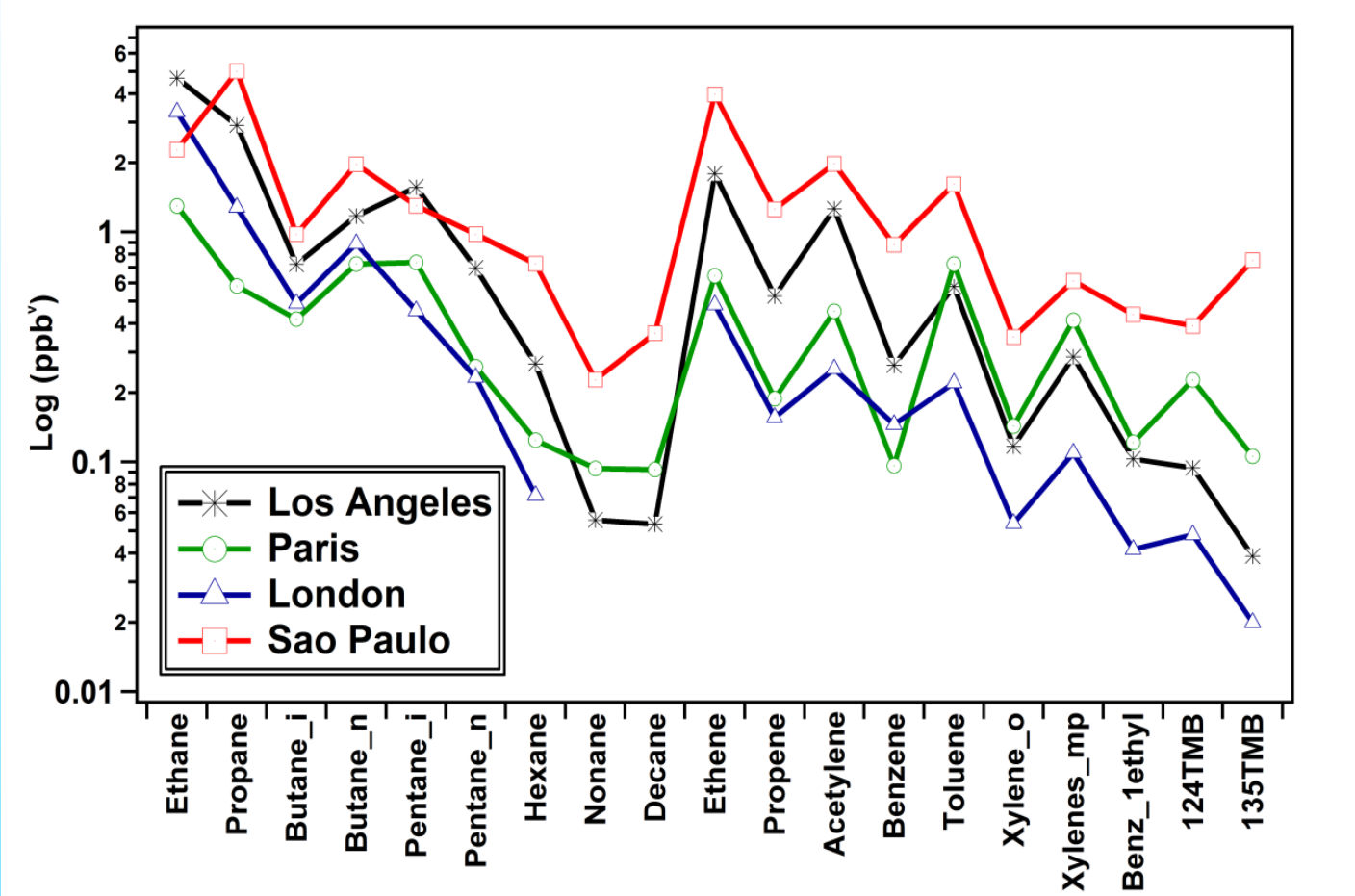

NMHCs average mixing ratios in São Paulo compared with those in other megacities.

Paris and London data were obtained in urban background air quality stations (Evry) (AIRPARIF, 2013) and London Eltham site (DEFRA, 2013), respectively). Los Angeles data were attained from CalNEx study in 2010 (ref) (CalNex, 2010).

Dominutti et al., 2016. Atmos. Environ.

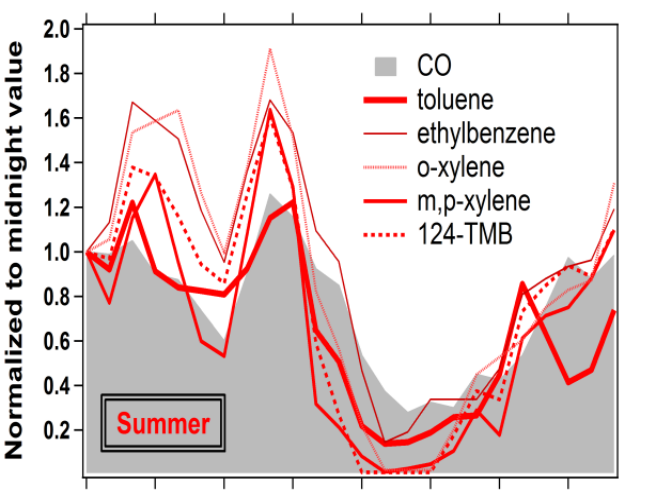

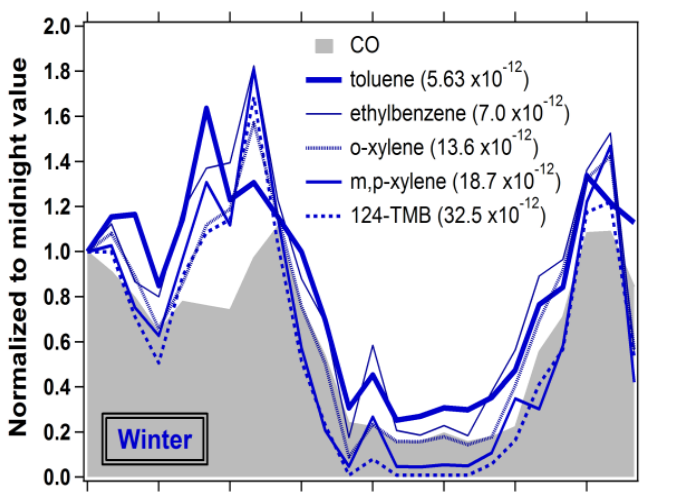

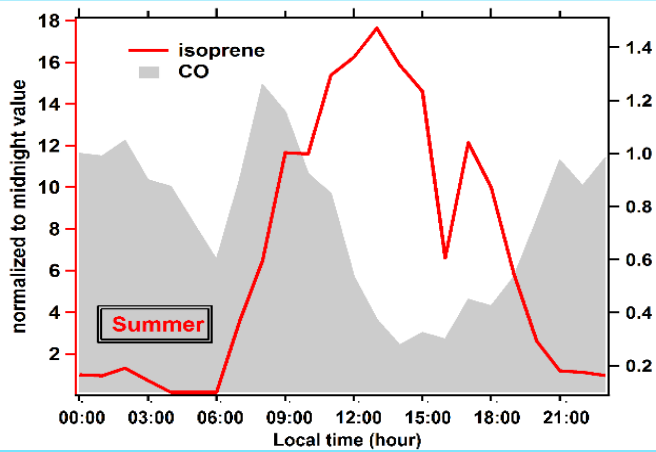

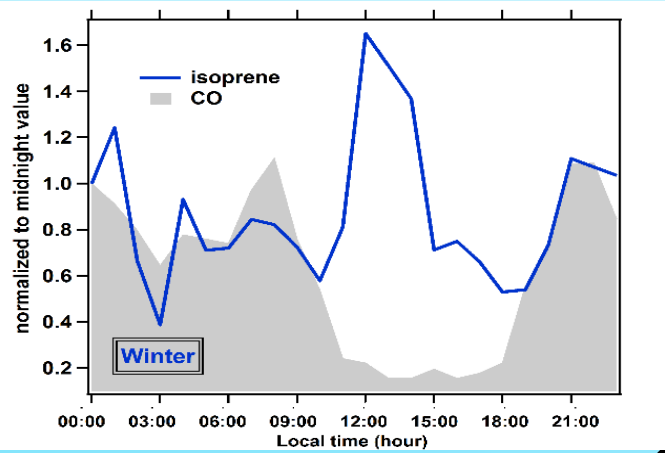

Normalized hourly profiles to midnight values of the mixing ratios of selected NMHCs and carbon monoxide (CO) during summer (red lines) and winter (blue lines) 2013.

Dominutti et al., 2016. Atmos. Environ.

OZONE PROFILE

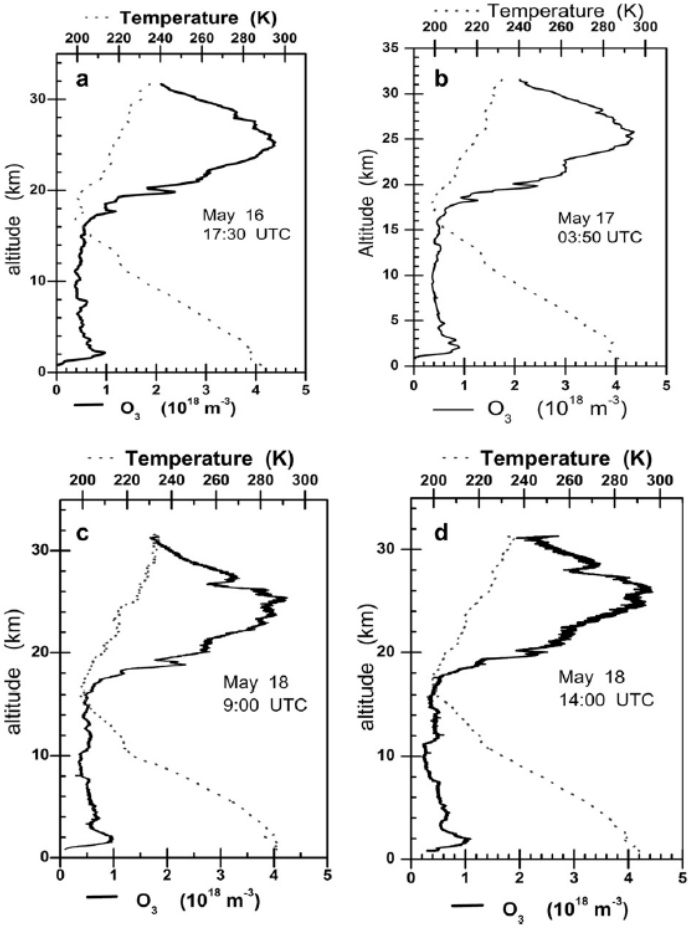

Fig. 3. Vertical profiles during the dry-season campaign: (a) 16 May, 17:30 UTC; (b) 17 May, 03:50 UTC; (c) 18 May, 09:00 UTC; (d) 18 May, 14:00 UTC. Ozone (ppb) in black and air temperature (K) in dark gray.

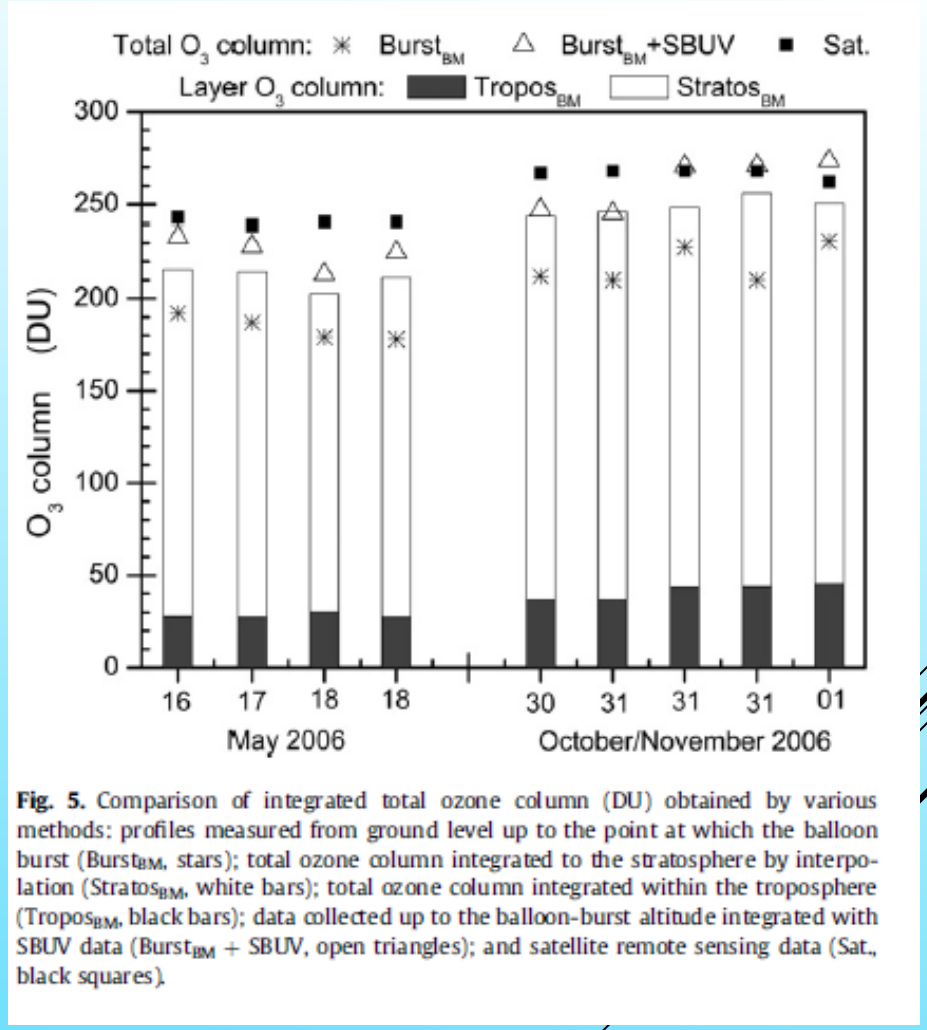

Fig. 5. Comparison of integrated total ozone column (DU) obtained by various methods: profiles measured from ground level up to the point at which the balloon burst ($Burst_{BM}$, stars); total ozone column integrated to the stratosphere by interpolation ($Stratos_{BM}$, white bars); total ozone column integrated within the troposphere ($Tropos_{BM}$, black bars); data collected up to the balloon-burst altitude integrated with SBUV data ($Burst_{BM}$ + SBUV, open triangles); and satellite remote sensing data (Sat., black squares).

Ozone sounding in the Metropolitan Area of São Paulo, Brazil: Wet and dry season campaigns of 2006

Evaluation of a superficial ozone concentration increase For 2000 to 2100

Prather et al., GRL 2003

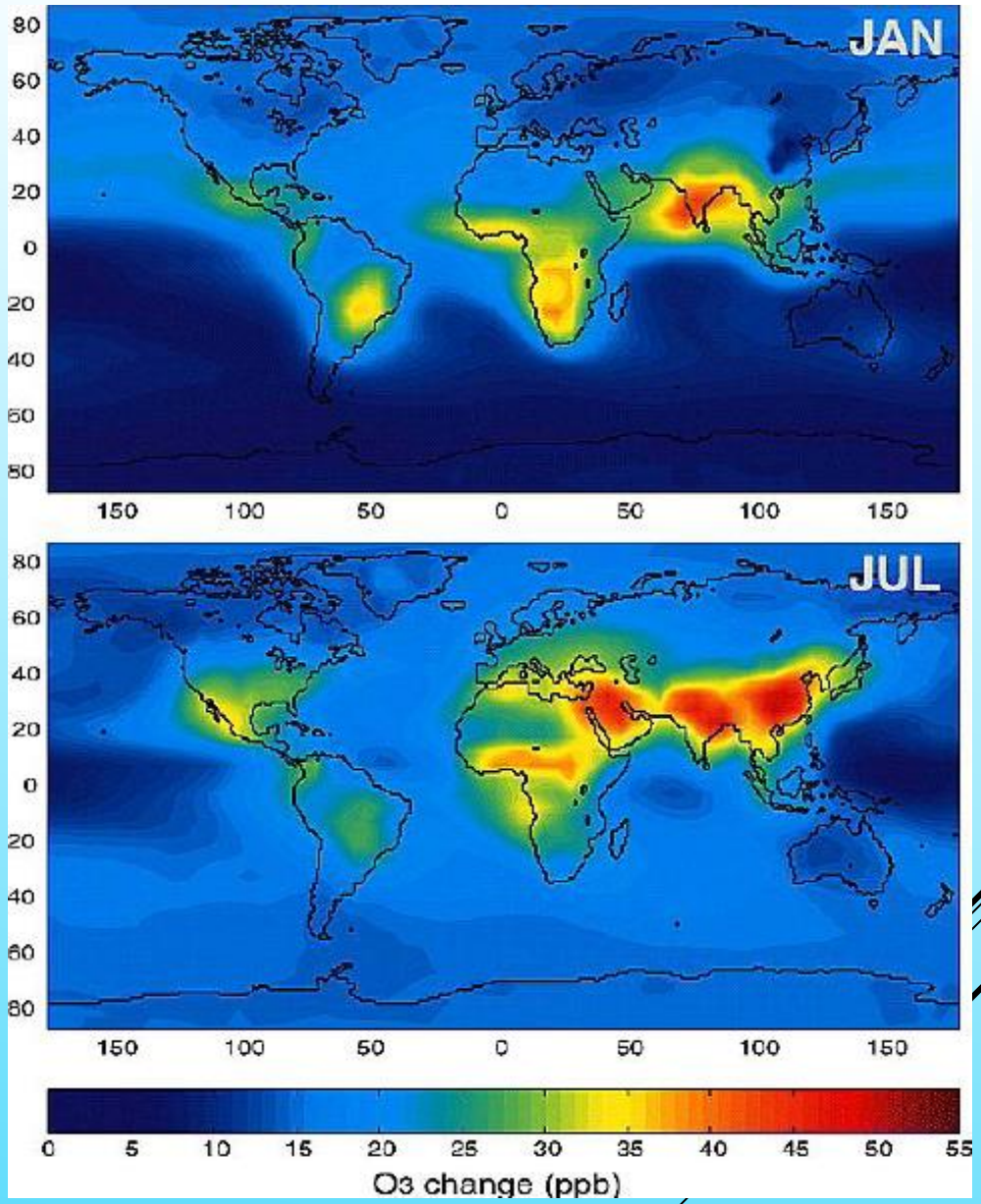

NMVOC↓

CH4↓

CO ↓

NOx ↓

CO ↓

NOx ↓

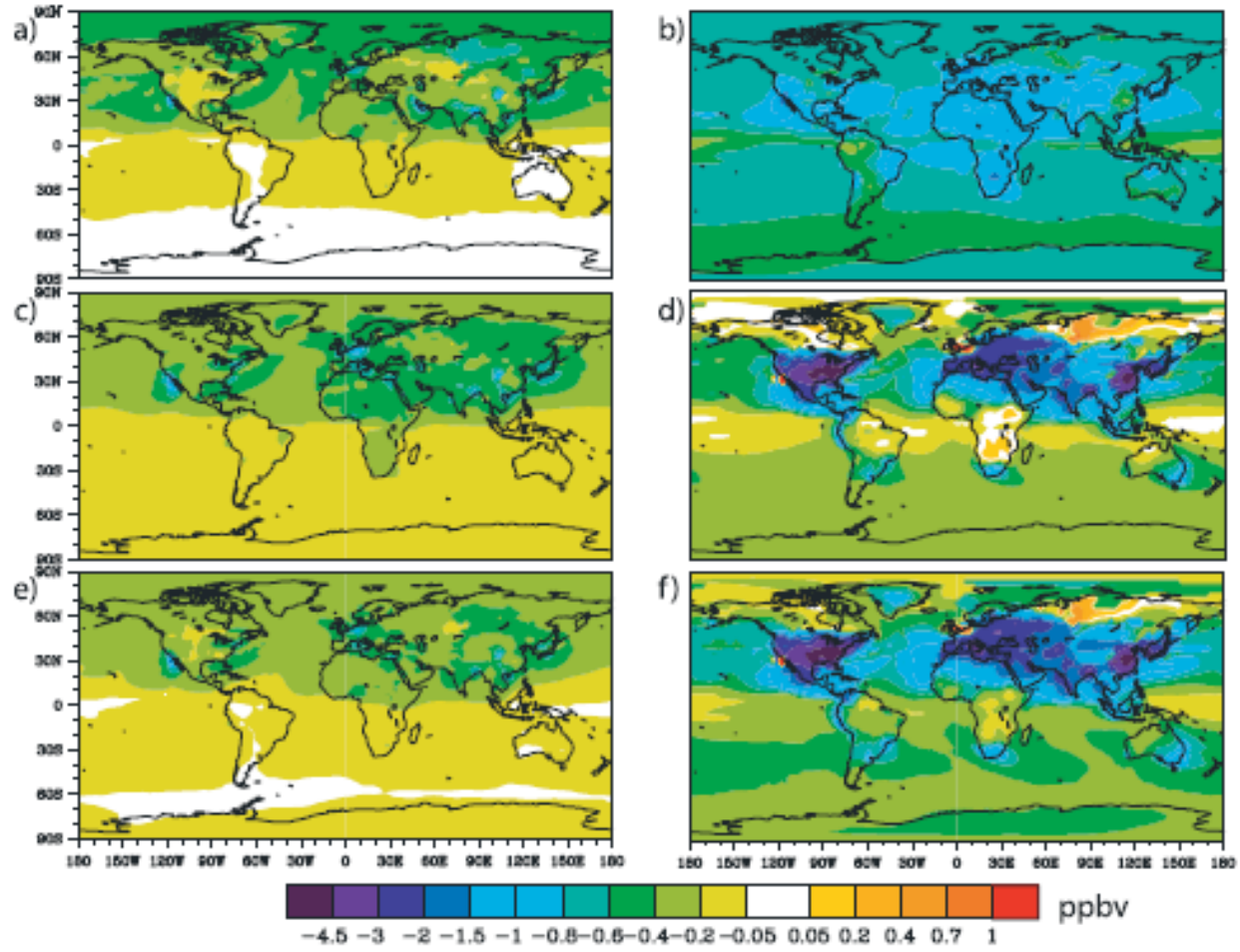

Figure 1. The change in 8-hr. daily maximum surface O_3 concentrations, averaged over the "O_3 season" (the three-month period with highest O_3 in each grid cell), due to 20% reductions in global anthropogenic emissions of O_3 precursors. Results are shown at steady state for (a) NMVOCs, (b) CH_4, (c) CO, and (d) NO_x, and short-term responses are shown for (e) CO and (f) NO_x. The short-term response for NMVOCs is nearly identical to the steady-state response.

WEST ET AL.: OZONE POLLUTION AND CLIMATE CONSEQUENCES

GEOPHYSICAL RESEARCH LETTERS, VOL. 34, L06806, doi:10.1029/2006GL029173, 2007

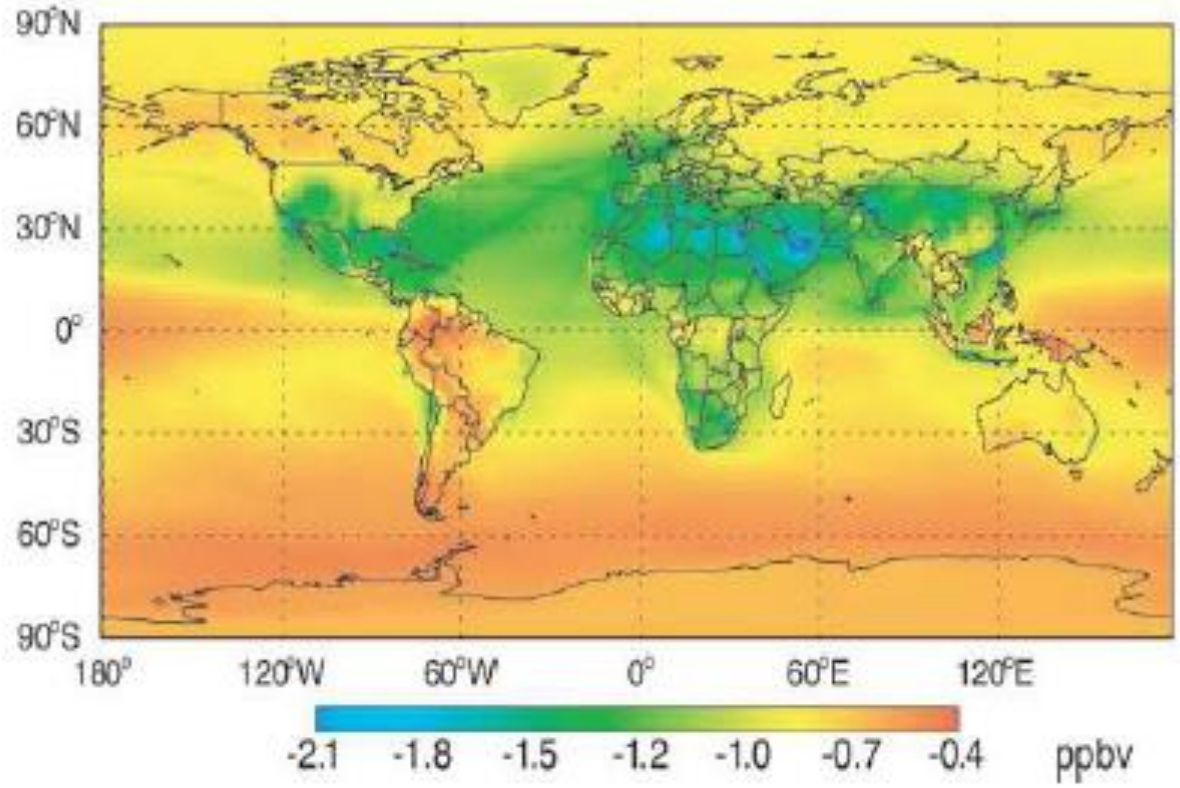

Figura N° 10. Change in annual average daily maximum 8-h surface O3 mixing ratios, at steady state, due to a 65 Mtyr reduction in CH4 emissions relative to the 2030 A2 base case (simulation IV minus III).

WEST ET AL.: OZONE POLLUTION AND CLIMATE CONSEQUENCES

GEOPHYSICAL RESEARCH LETTERS, VOL. 34, L06806, doi:10.1029/2006GL029173, 2007

- Scenarios

- 1- All the FLEX Fuel vehicles running with gasohol
- 2- All the Flex Fuel vehicles running with ethanol

IMPACT OF ETHANOL/GASOHOL ON OZONE FORMATION

Chamber Experiments

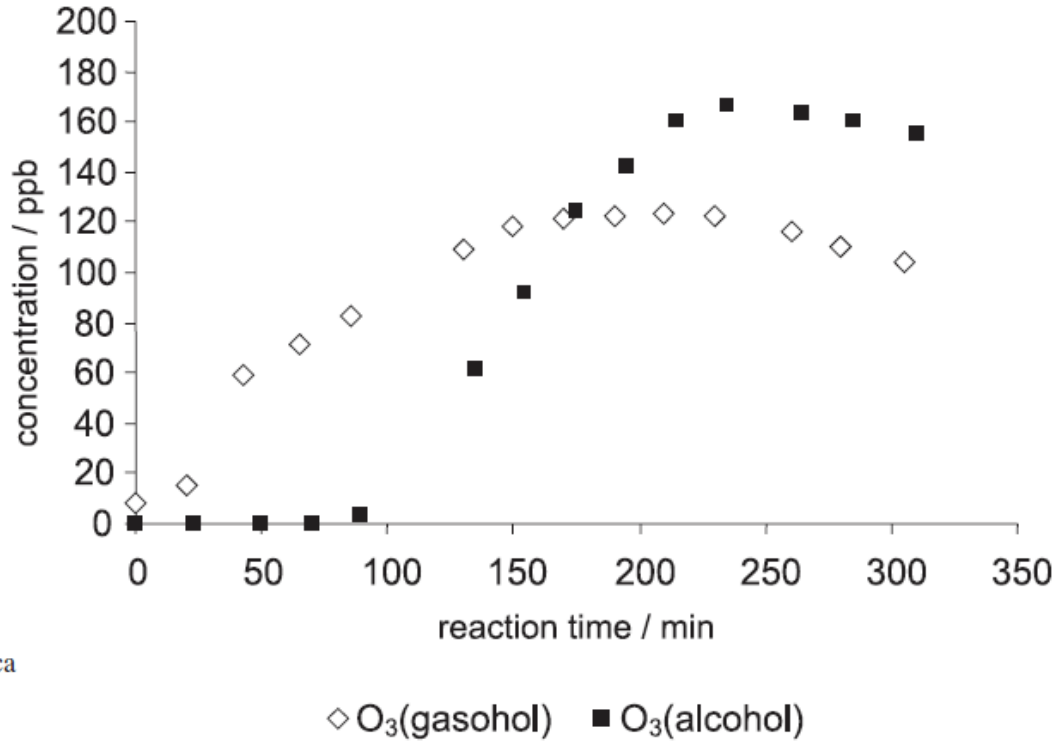

Figure 1. Typical ozone formation curves, obtained from exposures to sunlight of alcohol/NO- and gasohol/NO-mixtures.

J. Braz. Chem. Soc., Vol. 15, No. 5, 646-651, 2004.
Printed in Brazil - ©2004 Sociedade Brasileira de Química
0103 - 5053 $6.00+0.00

OTHER RESULTS:

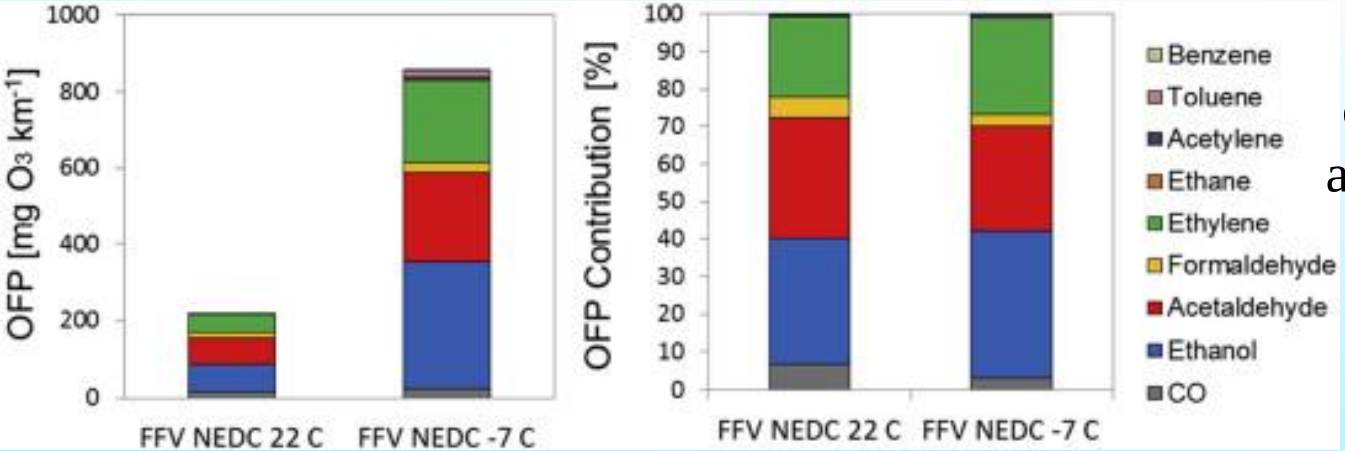

Estimated OFPs (mg O_3 km^{-1}) (left) and the percentage contributions (right) at 22 and −7 °C over the NEDC (New European Driving Cycle).

Emissions from a flex-fuel vehicle, fueled with E85 and E75, lead to SOA formation, from Oxygenated compounds.

R. Suarez-Bertoa et al. Primary emissions and secondary organic aerosol formation from the exhaust of a flex-fuel (ethanol) vehicle, In Atmospheric Environment, Volume 117, 2015, Pages 200-211,

Acetaldehyde, ethylene and their precursor, ethanol, were the main contributors to the OFP, accounting for up to 90% of the total at both temperatures.

As a consequence of increased use of ethanol fuel in Brazil, acetaldehyde, has become the fourth largest ozone precursor in some Brazilian areas

Formaldehyde and Acetaldehyde Concentrations in MASP

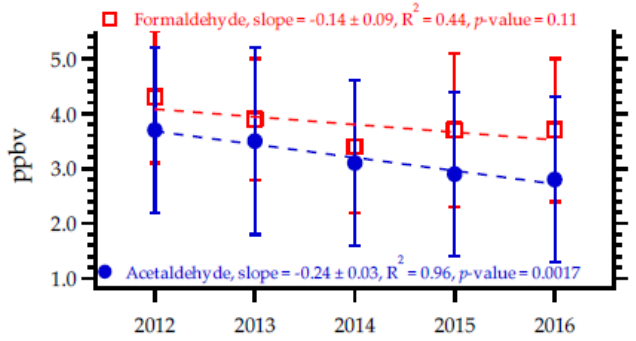

Figure 3. Annual trends in formaldehyde and acetaldehyde concentrations in the Metropolitan Area of São Paulo between 2012 and 2016. The dashed lines indicate the linear fit, and the bars indicate the bars indicate the standard deviation. Source: Pinheiros air quality monitoring station [24].

burn ethanol has increased (flex-fuel vehicles)

- The concentration of aldehydes has not increased (the use of ethanol has decreased)

Table 1
Environmental concentrations of formaldehyde and acetaldehyde in the MASP over the last 30 years.

Year	Formaldehyde (ppbv)	Acetaldehyde (ppbv)	F/A ratio	References
1986[a]	5.4	16.1	0.34	[52]
1989[a]	10.8	22.3	0.48	[21]
1990[a]	15.2	22.6	0.68	[21]
1993[a]	6.4	9.3	0.69	[21]
1996[a]	3.35	5.1	0.65	[21]
1997[a]	5.6	10.4	0.54	[21]
1998[a]	5.0	5.4	0.9	[53]
1999[b]	1.0–46	11.9	1.2	[54]
2000[a]	4.2		n.a.	[24]
2001[b]	1.0–46.3	1.2–56.6	n.a.	[47]
2002[a]	4.0		n.a.	[24]
2003[a]	2.0–8.2	1.0–9.2	0.9–3.2	[23]
2004[a]	18.1	15.4	1.18	[21]
2006[a]	5.7	5.6	1.02	[55]
2007[a]	13.5		n.a.	[24]
2011[a]	5.0	4.0	0.8–1.7	[22]
2012/2013	8.6 ± 6.7[c] 4.7[d]–6.9[e]–9.8[f]	5.4 ± 5.2[c] 2.3[d]–3.2[e]–6.5[f]	2.1 ± 1.3[c] 1.2[d]–1.8[e]–2.8[f]	Present study

[a] Mean values.
[b] Maximum and minimum values.
[c] Mean ± SD.
[d] 25th percentile.
[e] 50th percentile.
[f] 75th percentile.

Source: Formaldehyde and acetaldehyde measurements in urban atmosphere impacted by the use of ethanol biofuel: Metropolitan Area of Sao Paulo
Fuel, Nogueira et al., 2015

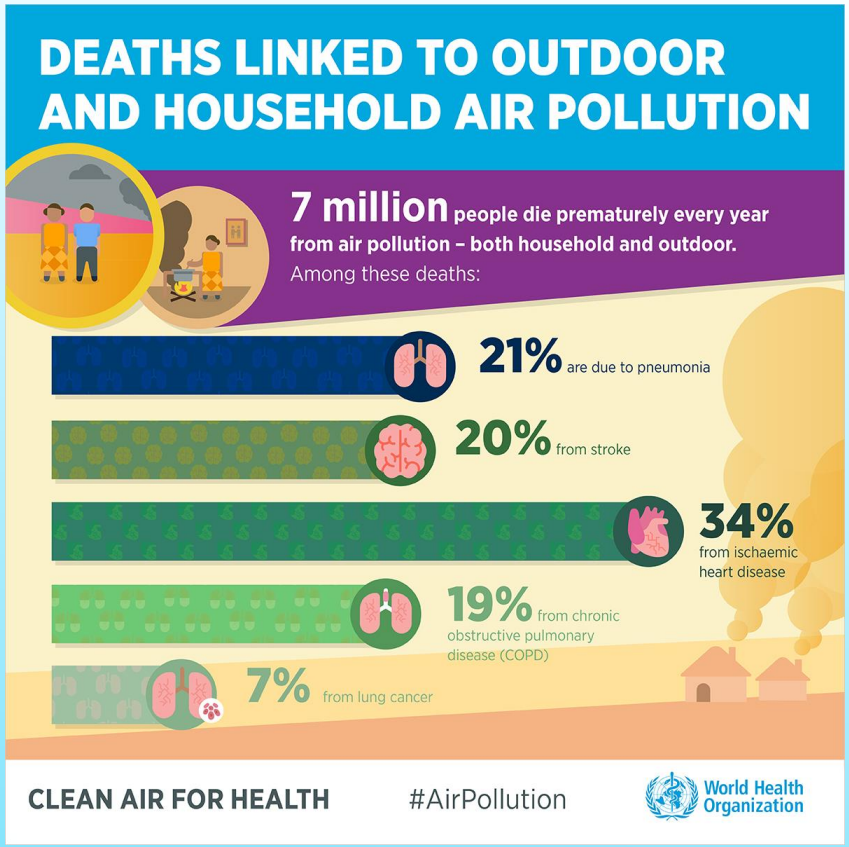

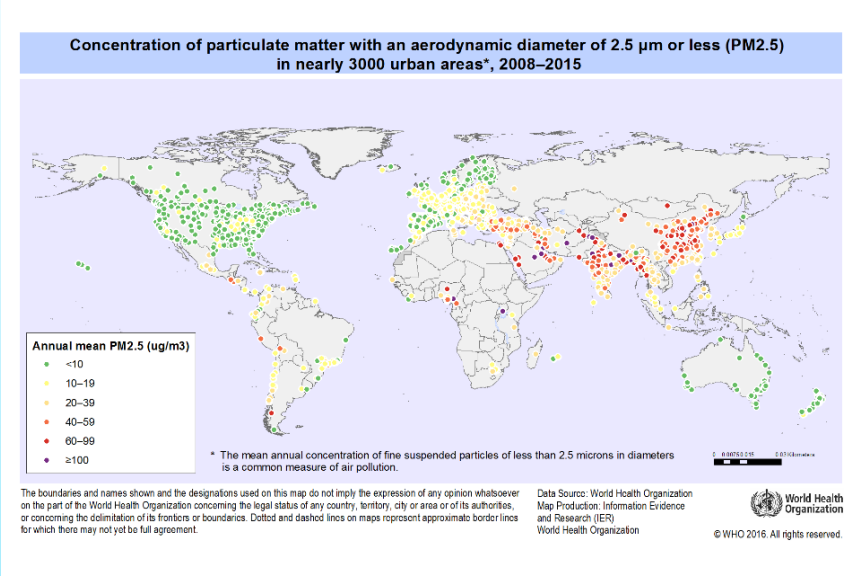

$PM_{2.5}$ – Particles with diameter less than 2.5 µm

INSTITUTO DE ASTRONOMIA, GEOFÍSICA E CIÊNCIAS ATMOSFÉRICAS
USP Universidade de São Paulo

SECONDARY ORGANIC AEROSOL (SOA)

SECONDARY INORGANIC AEROSOL (SIA)

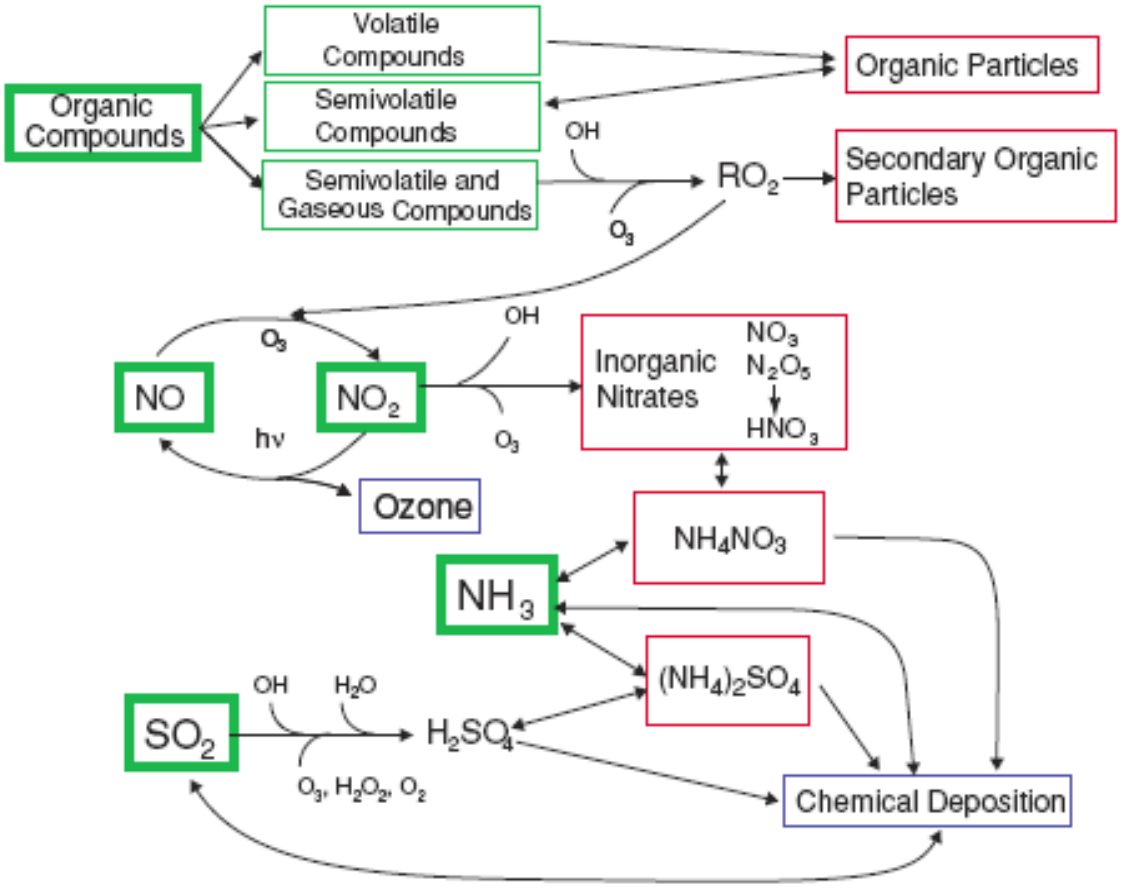

Chemical links between Ozone and PM formation

SECONDARY ORGANIC AEROSOL (SOA)
PRIMARY BIOLOGICAL AEROSOL PARTICLES (PBAP)

Sulfate Organics

[Zhang et al., 2007]

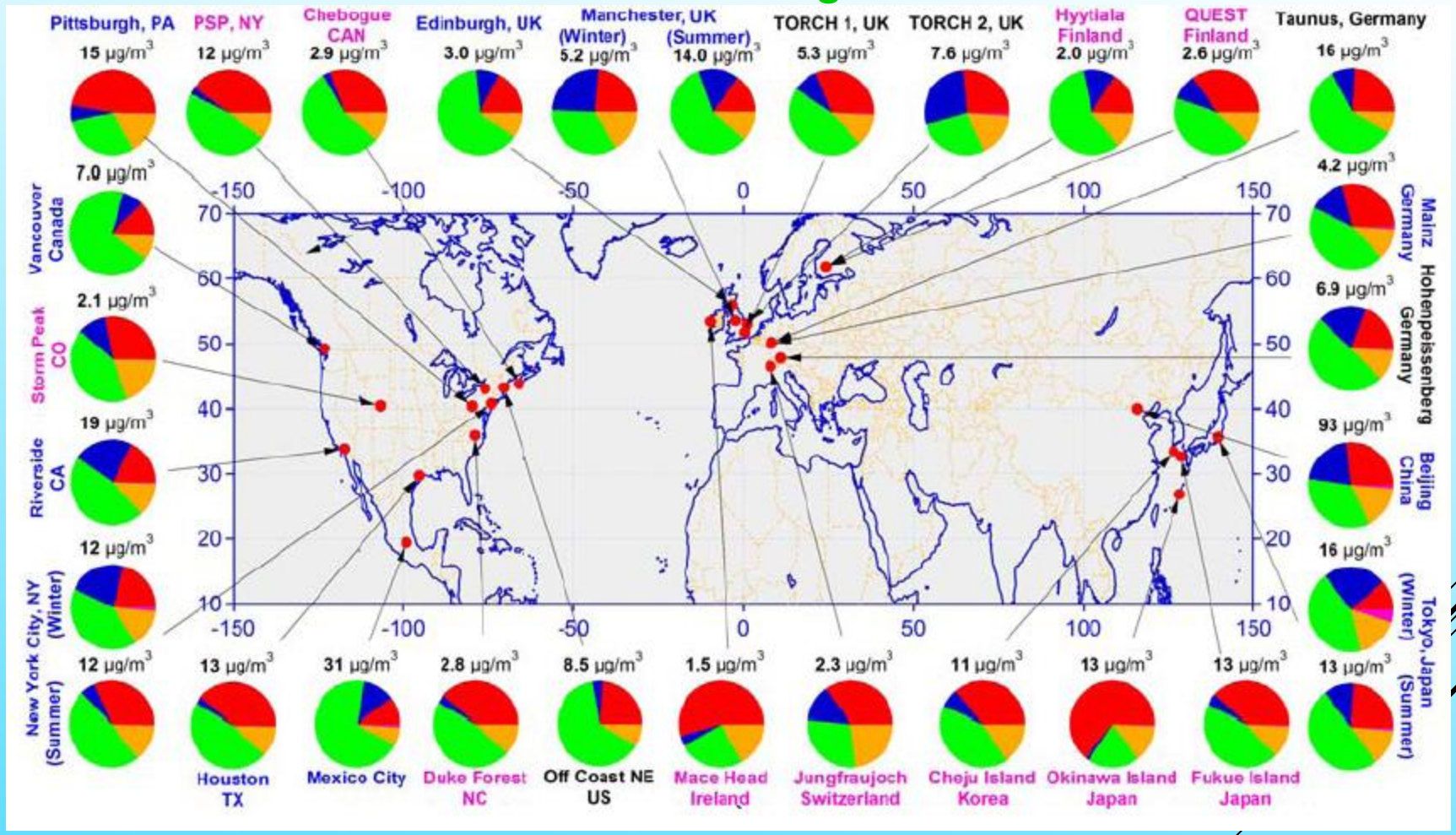

- Organic material contributes 20-50% of the total fine aerosol mass at continental mid-latitudes [Saxena and Hildemann, 1996; Putaud et al., 2004] and as much as 90% in the tropical forested areas [Andreae and Crutzen, 1997; Talbot et al., 1988; 1990; Artaxo et al., 1988; 1990; Roberts et al., 2001]

Black Carbon
Black carbon climate danger "underestimated",

Black carbon, is very important in a global scale,

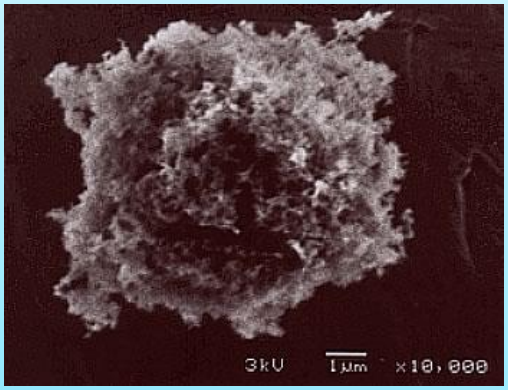

Studies showed that Black Carbon can be the second major responsible for the global warming, being behind only for CO_2.

Ramanathan &Carmichael
Nature Geoscience 1, 221 (2008)

CLIMATE CHANGE

Aerosols heat up

NATURE|Vol 448|2 August 2007

Peter Pilewskie

Solid particles suspended in the atmosphere have long played second fiddle to greenhouse gases as agents of climate change. A study of atmospheric heating over the Indian Ocean could provoke a rethink.

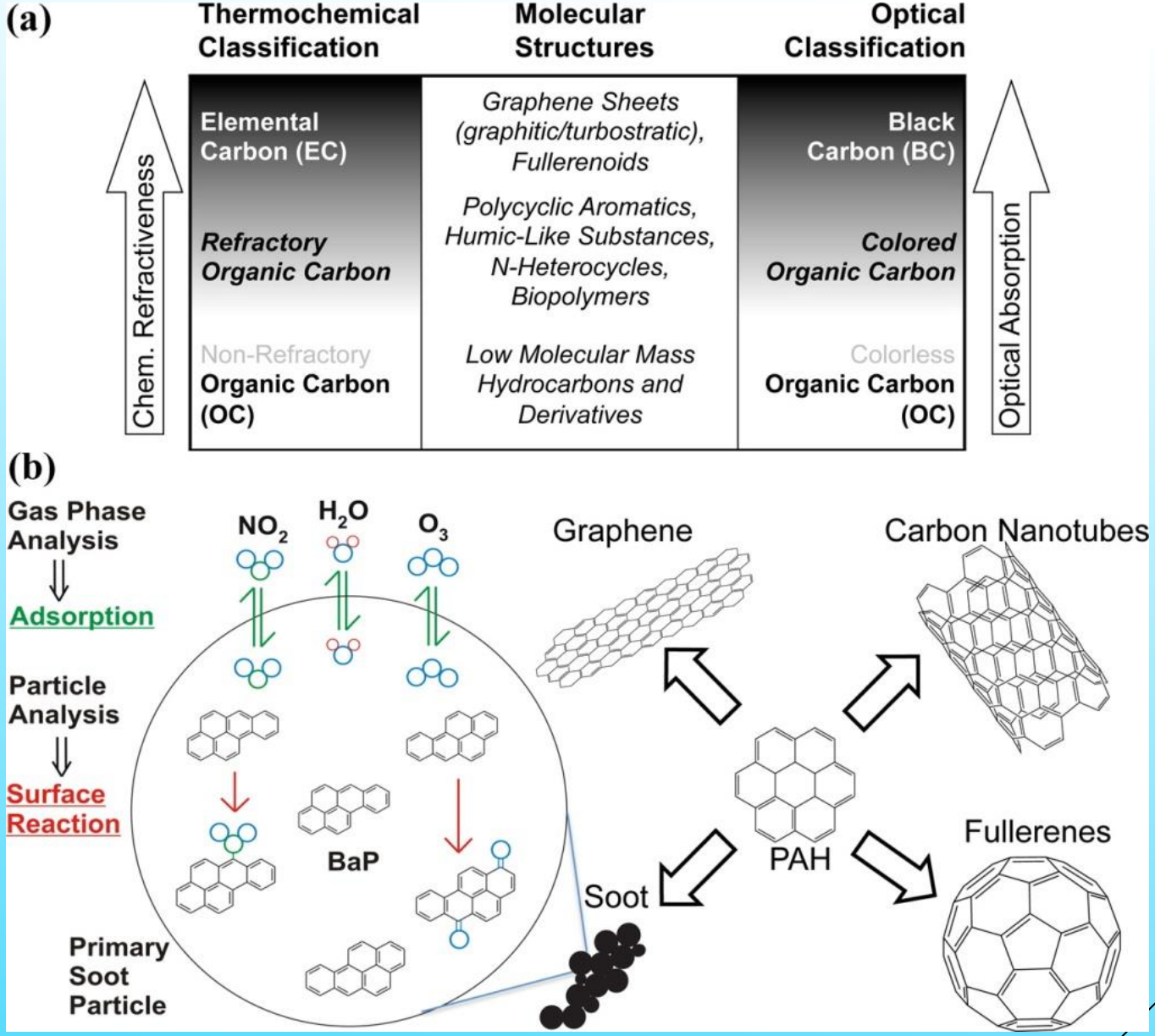

Ulrich Pöschl; Manabu Shiraiwa; *Chem. Rev.* **2015,** 115, 4440-4475.

Emission Inventory of Organic Aerosols

Botton-up approach

BSOA (biogenic SOA)	12-70 TgC/year
POA	35 TgC/year (9 anthropogenic) (25 biomass burning)
ASOA	2- 12 TgC/year
Total	50-90 TgC/year

The formation, properties and impact of secondary organic aerosol: current and emerging issues

Atmos. Chem. Phys., 9, 5155–5236, 2009 www.atmos-chem-phys.net/9/5155/2009/

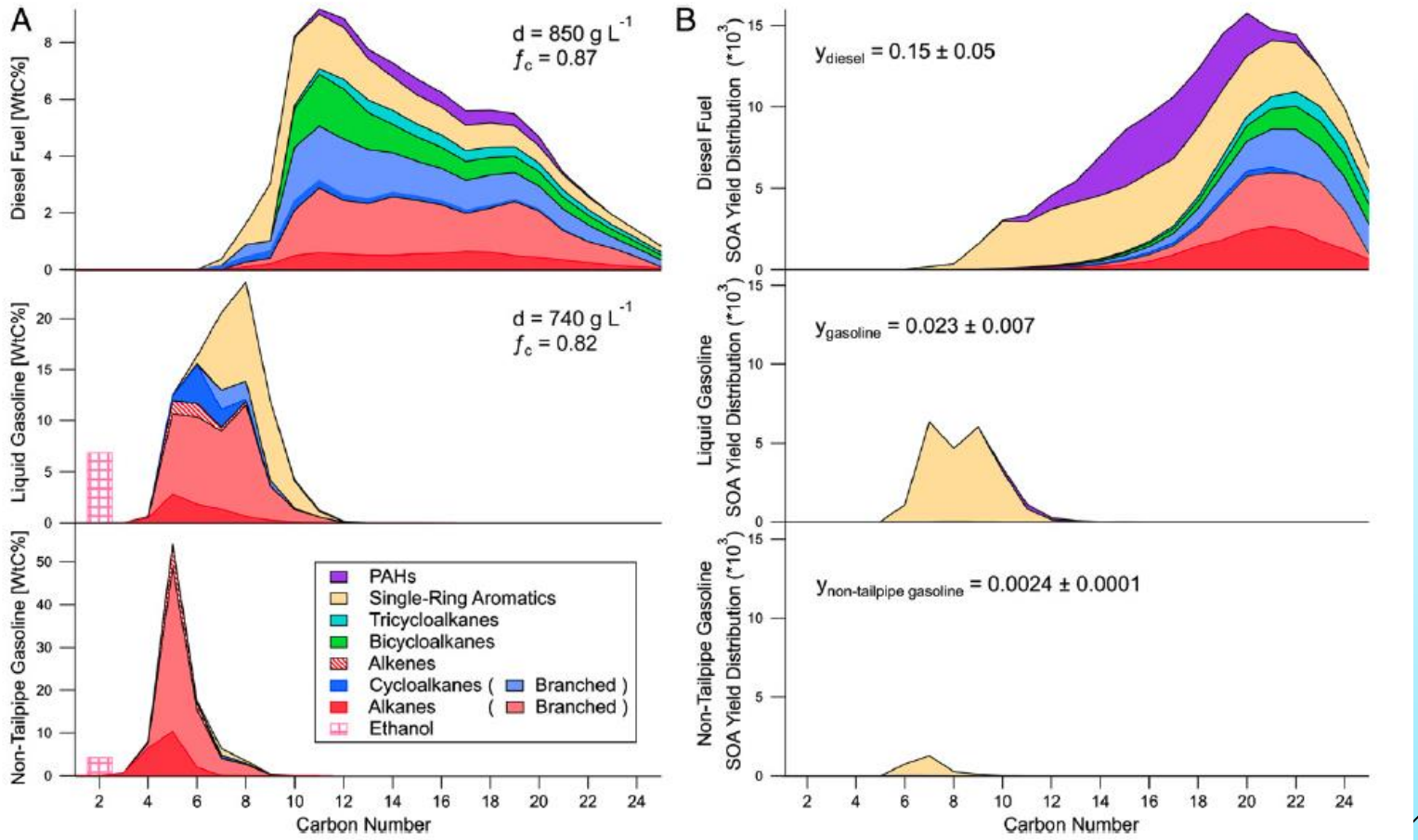

Fig. 2. Distribution of mass (*A*) and SOA formation potential (in μg SOA·μg^{-1}; *B*) in diesel and gasoline fuel (representative of exhaust) and nontailpipe gasoline emissions. Distributions in *A* and *B* are colored by chemical class. Fuel properties (density, carbon fraction) and bulk SOA yields (at an organic particle loading of 10 μg·m^{-3}) are superposed on *A* and *B*, respectively. Predicted SOA from gasoline exhaust is much lower than diesel and dominated solely by aromatic content, whereas diesel SOA is produced from a mix of aromatic and aliphatic compounds. A distribution of the SOA potential uncertainties is provided in *SI Appendix*, Fig. S5.

Elucidating secondary organic aerosol from diesel and gasoline vehicles through detailed characterization of organic carbon emissions

Drew R. Gentner[a], Gabriel Isaacman[b], David R. Worton[b,c], Arthur W. H. Chan[b], Timothy R. Dallmann[a], Laura Davis[a], Shang Liu[d], Douglas A. Day[d,1], Lynn M. Russell[d], Kevin R. Wilson[e], Robin Weber[b], Abhinav Guha[b], Robert A. Harley[a], and Allen H. Goldstein[a,b,2]

18318–18323 | PNAS | November 6, 2012 | vol. 109 | no. 45

Table 1. Distribution of mass and SOA potential by chemical class for diesel exhaust, gasoline exhaust, and nontailpipe gasoline

Compound class	Weight by carbon, wtC%			Potential SOA formation, wt%		
	Diesel exhaust	Gasoline exhaust	Non-tailpipe gasoline	Diesel exhaust	Gasoline exhaust	Non-tailpipe gasoline
Total aliphatic	68 ± 8	58 ± 2	85 ± 4	47 ± 4	0.38 ± 0.07	0.9 ± 0.4
Straight-chain alkanes	7 ± 1	7.7 ± 0.3	20 ± 1	11 ± 2	0.09 ± 0.003	0.02 ± 0.001
Branched alkanes	23 ± 2	40 ± 1	60 ± 3	14 ± 2	0.12 ± 0.003	0.13 ± 0.01
Cycloalkanes (single straight alkyl chain)	2.5 ± 0.2	4.3 ± 0.1	1.03 ± 0.04	1.2 ± 0.3	0.13 ± 0.07	0.7 ± 0.4
Cycloalkanes [branched/multiple alkyl chain(s)]	18 ± 2	6.2 ± 0.3	5.0 ± 0.2	11 ± 2	0.04 ± 0.02	0.05 ± 0.03
Bicycloalkanes	13 ± 1	0	0	6 ± 1	0	0
Tricycloalkanes	4.8 ± 0.6	0	0	4 ± 1	0	0
Single-ring aromatics	19 ± 2	29 ± 1	2.7 ± 0.1	36 ± 9	96 ± 22	99 ± 6
Polycyclic aromatic compounds	4 ± 2	0.32 ± 0.02	0.0003	17 ± 8	3.2 ± 0.9	0.01 ± 0.01
Alkenes (straight, branched, cyclic)	0	3.6 ± 0.1	7.4 ± 0.3	0	0	0
Ethanol	0	6.9 ± 0.5	4.4 ± 0.4	0	0	0

The wt% by total mass for each source can be found in the *SI Appendix*, Table S2.

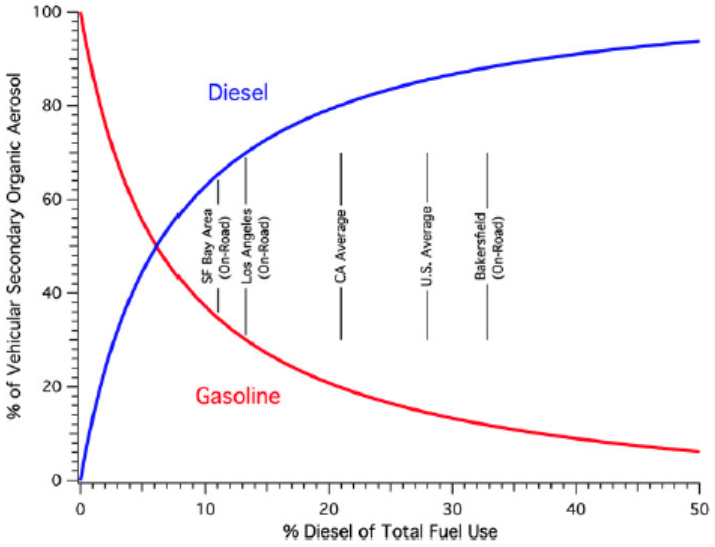

Fig. 3. The percent contribution of gasoline and diesel exhaust to SOA over 0% to 50% diesel fuel use demonstrates the predominance of diesel sources for SOA formation. SOA contributions form the two sources are equivalent at 6% diesel fuel use. The United States and California state averages shown are based on total on- and off-road use. The urban areas in California shown are for on-road fuel use only; off-road contributions will increase the diesel fraction of total use by several percent, but are not available at this scale.

Elucidating secondary organic aerosol from diesel and gasoline vehicles through detailed characterization of organic carbon emissions

Drew R. Gentner[a], Gabriel Isaacman[b], David R. Worton[b,c], Arthur W. H. Chan[b], Timothy R. Dallmann[a], Laura Davis[a], Shang Liu[d], Douglas A. Day[d,1], Lynn M. Russell[d], Kevin R. Wilson[e], Robin Weber[b], Abhinav Guha[b], Robert A. Harley[a], and Allen H. Goldstein[a,b,2]

PRIMARY BIOLOGICAL AEROSOL PARTICLES (PBAP)

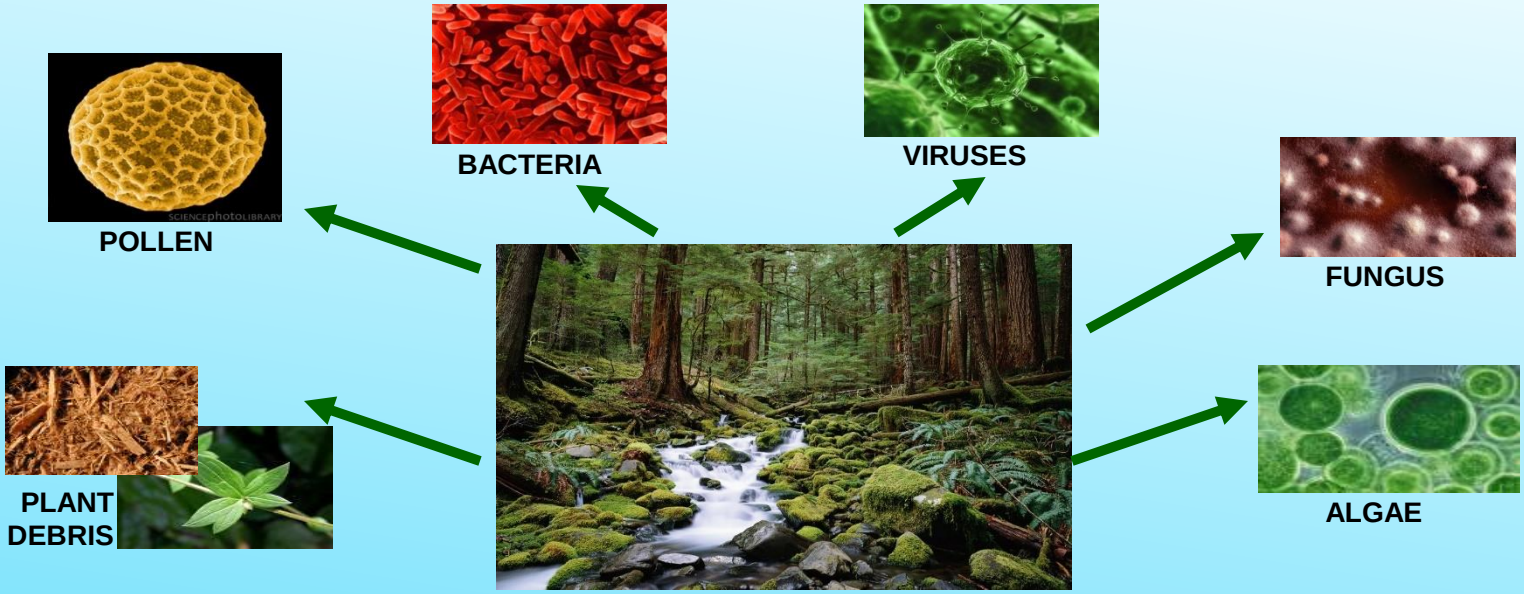

Jaenicke [2005] suggests may be as large a source as dust/sea salt (1000s Tg/yr)

May act as CCN and IN [*Diehl et al*., 2001; *Bauer et al.,* 2003; *Christiner et al.,* 2008]

SOUTH AMERICA

Latin America and the Caribbean Population

- 648,476,231 (in 2017 according to United Nations)

- Latin America and the Caribbean population is equivalent to 8.62% of the total world population.
- The population density in Latin America and the Caribbean is 32 per Km^2 (83 people per mi^2).
- The total land area is 20,158,154 Km^2 (7,783,104 sq. miles)
- 79.7 % of the population is urban (516,362,188 people in 2017)
- The median age in Latin America and the Caribbean is 29.6 years.

Worldometers (http://www.worldometers.info/world-population/latin-america-and-the-caribbean-population/)

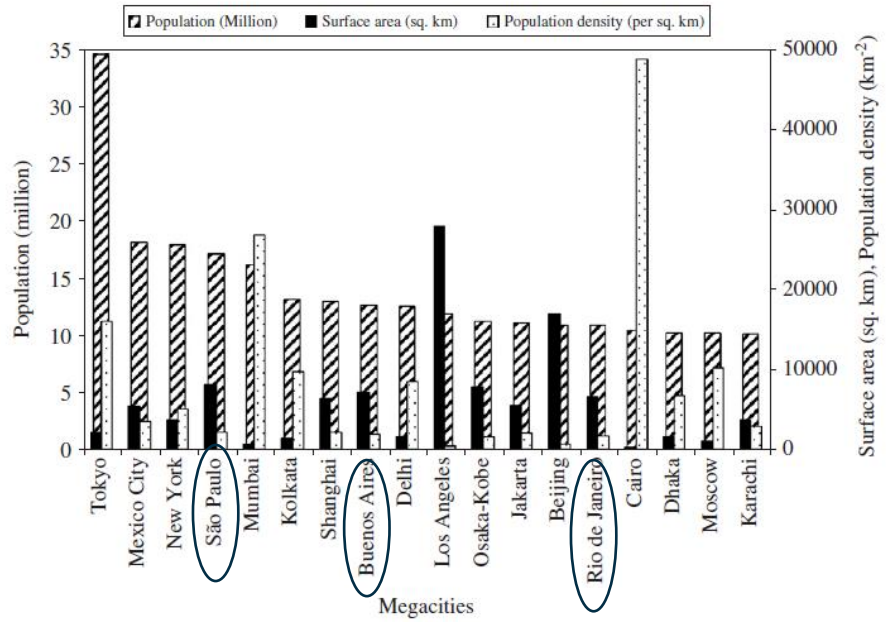

. Megacity population (million), surface area (km^2), and population density (number of people per km^2) in 2000.

Evaluation of emissions and air quality in megacities

B.R. Gurjar[a,*], T.M. Butler[b], M.G. Lawrence[b], J. Lelieveld[b]

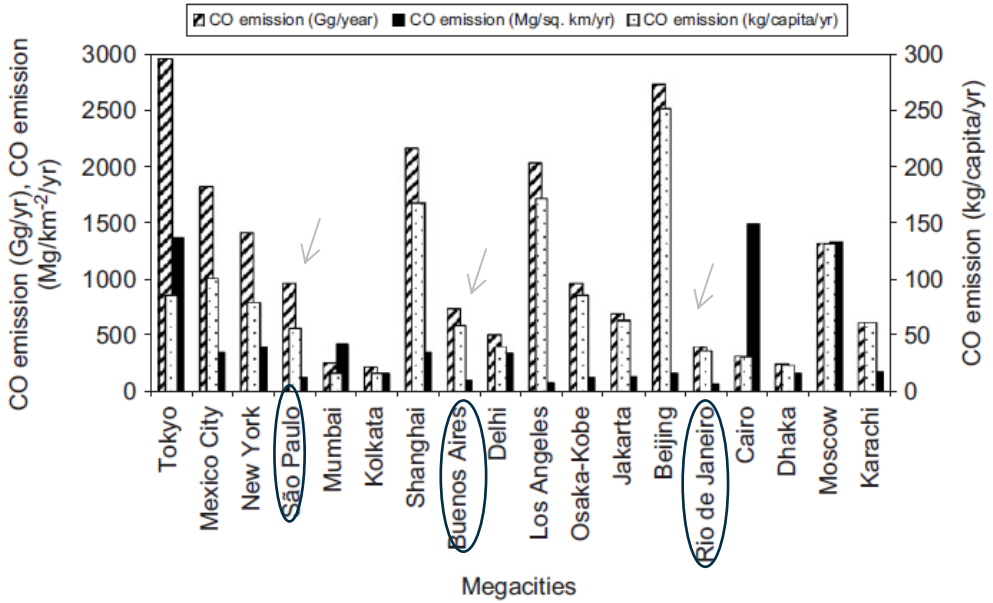

Fig. 2. Annual CO emission estimates for 2000 (Gg year^{-1}).

Metropolitan Area of São Paulo - MASP

MASP= São Paulo city + 38 cities

- 21 million inhabitants
- 7,2 million vehicles
- 2000 significative industrial plants
- 8000 km^2

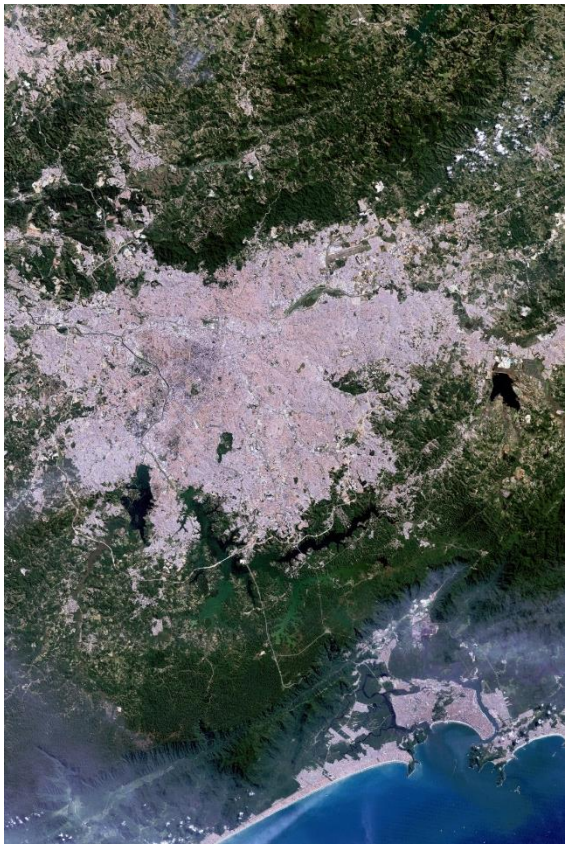

Characterization of the air Pollution Problem

New Directions: from biofuels to wood stoves: the modern and ancient air quality challanges in the megacity of São Paulo. Atmos. Environ., 2016

MASP (Metropolitan Area of São Paulo)

Population:~ 21 million inhabitants.

Area: 8511 km^2

Vehicle fleet: 7 million passenger and commercial vehicles

85% light-duty vehicles (LDVs)

- 31 % of LDVs use gasohol (75% gasoline +25% ethanol)
- 2 % use hydrous ethanol (95% ethanol +5% water)
- 50 % are flex-fuel (any proportion of gasohol or ethanol)
- 2% use diesel (diesel with 8% biofuel)

3% heavy-duty diesel vehicles (HDVs)

12% motorcycles

- **Ethanol represents 55% of the burned fuel.**
- **50% of the cars have more than 10 years of use.**

Evolution of the average values of CO, PM_{10}, O_3, SO_2 and NO_2 concentrations measured at the CETESB air quality monitoring stations in the MASP

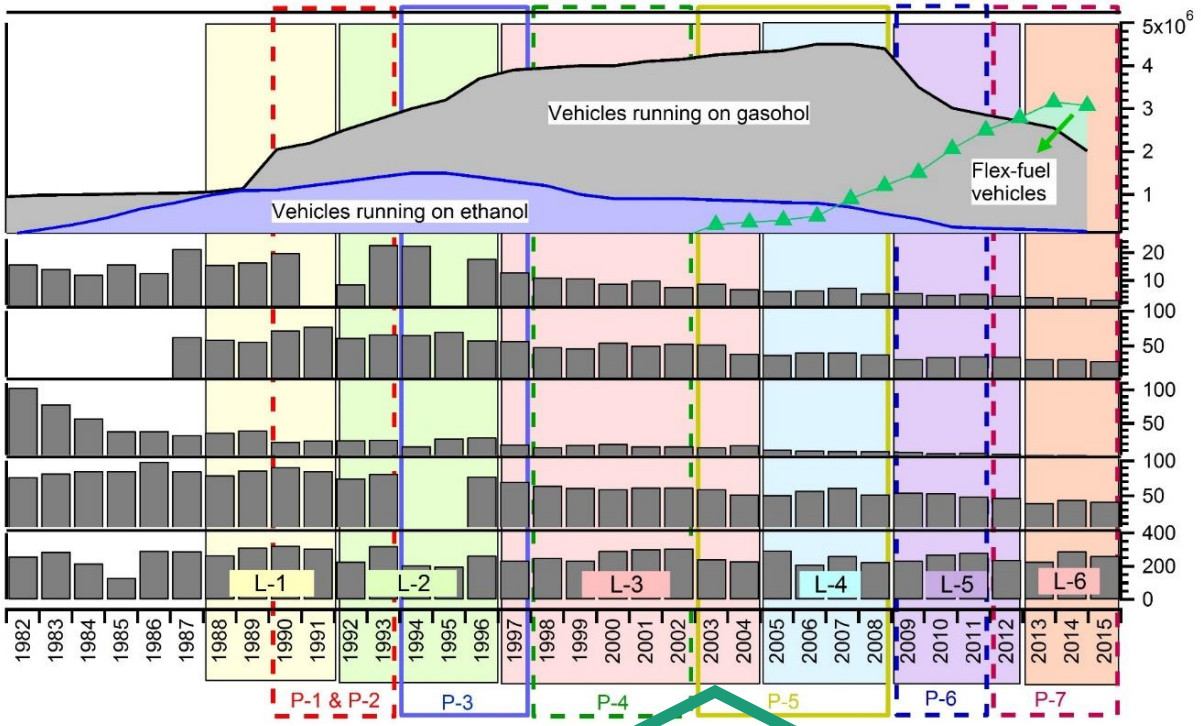

PROMOT: PROGRAM FOR CONTROLLING THE EMISSIONS BY MOTORCYCLES

Established in 2003 for regulation of motorcycles emission.

PROCONVE: PROGRAM FOR CONTROLLING THE VEHICULAR EMISSIONS

Established in 1983 for light and heavy-duty vehicles

Source: Air quality in the megacity of Sao Paulo: evolution over the last 30 years and future perspectives. Atmos. Environ., 2017

Sources not properly accounted

- Evaporative emissions during refuelling
- Solvents: painting and industries
- Biomass burning
  - Vegetation residues
  - Wood, charcoal

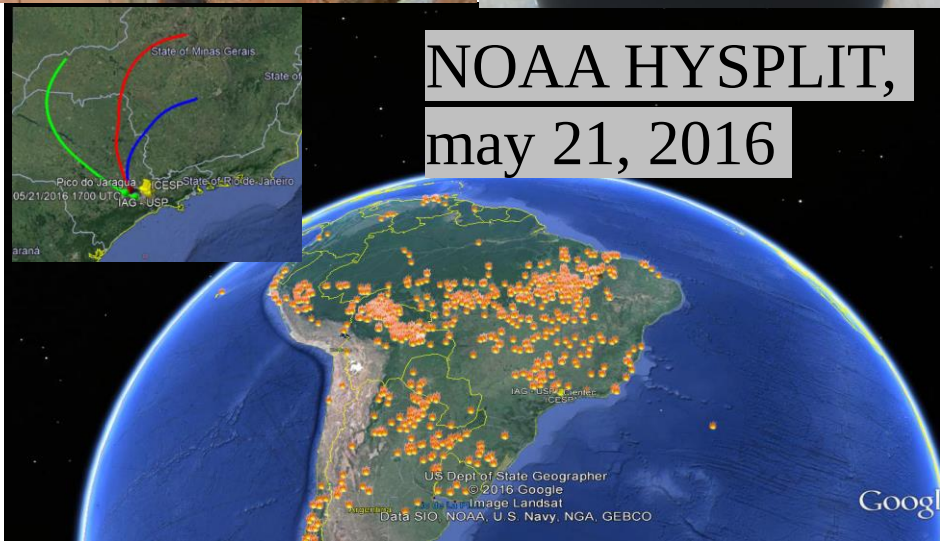

NOAA HYSPLIT, may 21, 2016

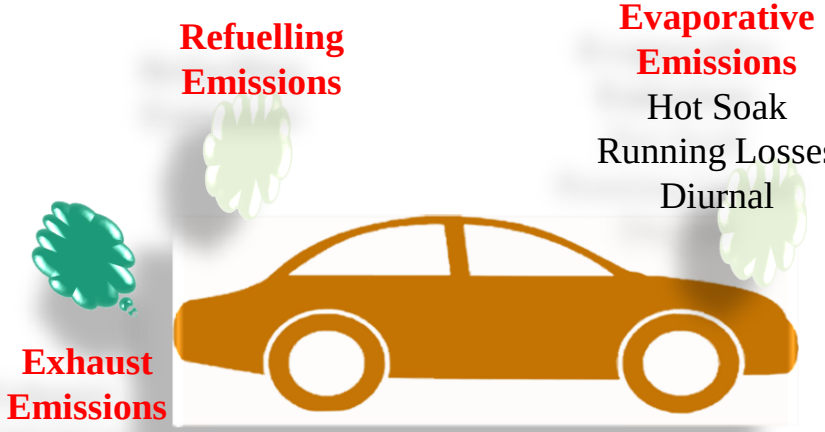

Vehicular Emissions

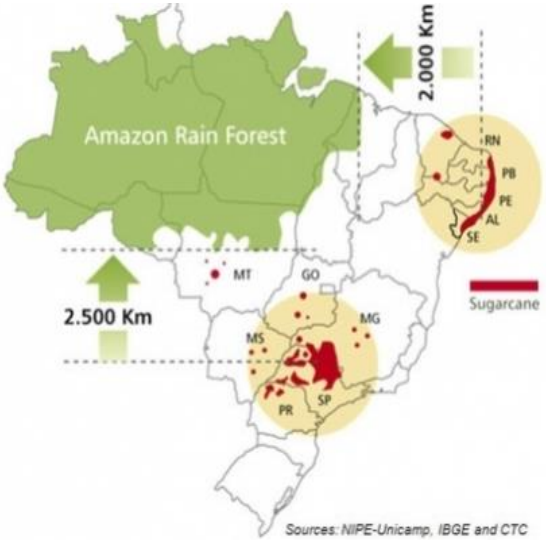

Air pollution in Sao Paulo MegaCity

who is more impacted?

PROGRAMS TO CONTROL EMISSIONS REDUCED THE AVERAGE CONCENTRATION

BUT STILL HOT SPOTS OF CONCENTRATION AFFECT THE POPULATION

TWO ASPECTS: TIME SPEND TO COMMUTE AND INEQUALITY IN ACCESS TO TRANSPORT

POPULATION EXPOSURE DUE TO HOT SPOTS OF POLLUTION, INEQUALITY EXPOSURE

- The air we breathe is different from place to place
- The air quality is very variable in the same city
- The concentration of pollutants varies according to site, hour and season
- The climate change will impact the air quality mainly in the megacities.

Mean annual concentrations of trace elements (in ng/m3) present in the $PM_{2.5}$ (in $\mu g/m^3$). The measurements were performed during different experimental campaigns and at different locations in the MASP.

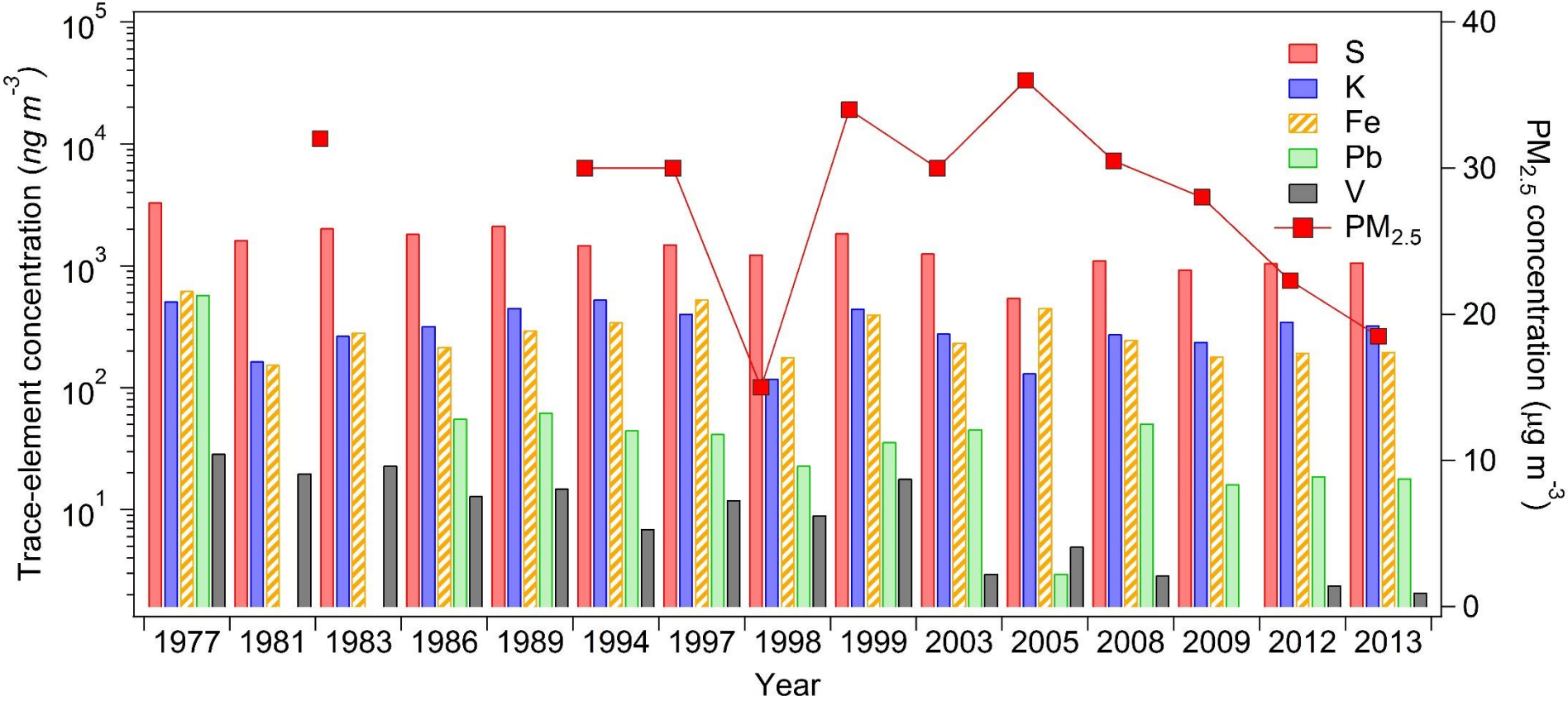

$OC/PM_{2.5}$= 0.55
$EC/PM_{2.5}$= 0.20

Air quality in the megacity of Sao Paulo: evolution over the last 30 years and future perspectives. Atmos. Environ., 2017

Carbonaceous aerosols in MASP

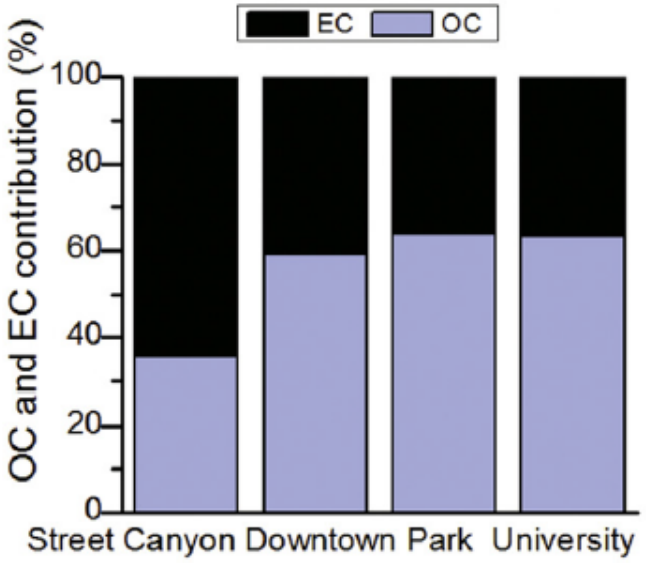

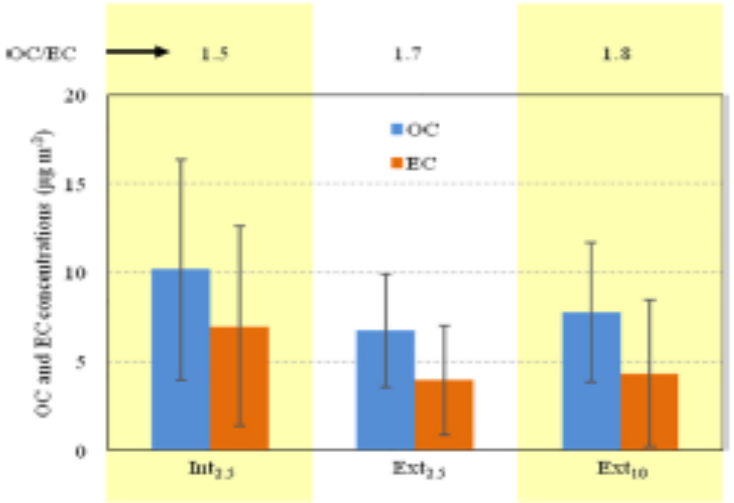

Figure 4. Carbonaceous species concentrations for all campaigns.

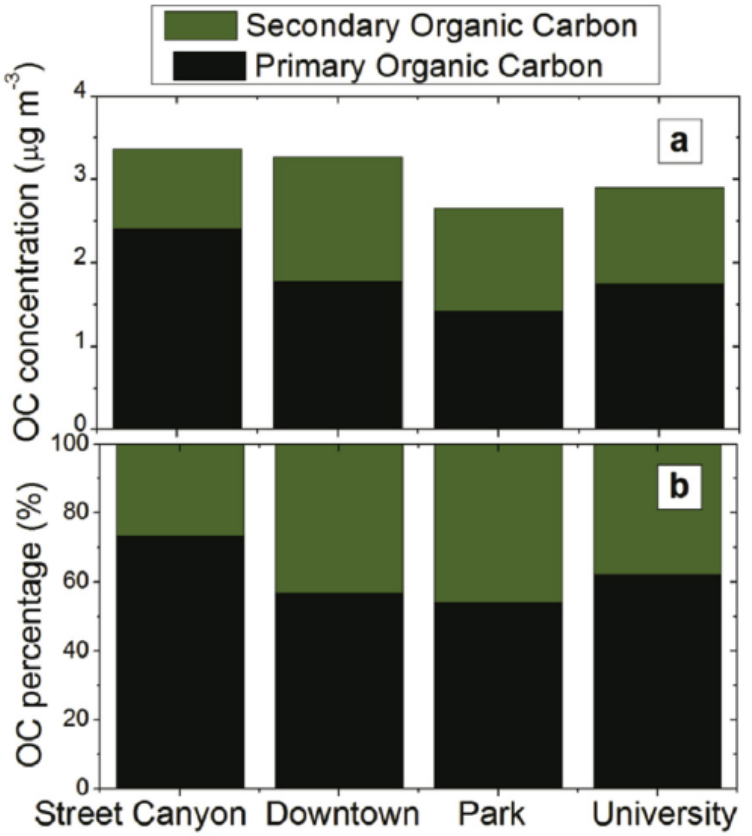

Fig. 4. Average concentration and percentage of total OC attributable to the estimated secondary and primary organic carbon at Street Canyon, Downtown, Park and University sites.

Santos et al., Atmos. Environ, 2016

Pereira et al., ACP, 2017

References:
1) Ke Lia, Daniel J. Jacob, Hong Liaoa, Lu Shen, Qiang Zhang, and Kelvin H. Bates. Anthropogenic drivers of 2013–2017 trends in summer surface ozone in China. PNAS, January 8, 2019, vol. 116, no. 2
2) WMO/IGAC Impacts of Megacities on
Air Pollution and Climate. Website:
http://www.wmo.int/pages/prog/arep/gaw/gaw_home_en.html
3) Miriam E. Marlier1,2 & Amir S. Jina3 & Patrick L. Kinney4 & Ruth S. DeFries. Extreme Air Pollution in Global Megacities. Curr Clim Change Rep (2016) 2:15–27
4) Baumgardner, M de Fatima Andrade, Z Klimont, J Kuylenstierna, SM Carvalho, N Borgford-Parnell, OL Mayol-Bracero, M Melamed, R Seguel, M Andrade, C Rudamas, G Ruiz-Suárez, O Sanchez-Ccoyllo, J Ometto, M Cazorla, L Höglund Isaksson, P Purohit, OM Cerutti, P Medina, N Hununeeus, JA Ortinez, L Dawidowski, D Henze, N Roja. Short-lived climate pollutants: Drivers, regional emissions and measurements, 2018.

Obrigada!
THANK YOU!

Acknowledgements